Journal of Medicinal Chemistry Article

J. Med. Chem. **2010,** *53,* 5449–5466 **5449**
DOI: 10.1021/jm1000584

Structural Optimization and Biological Evaluation of Substituted Bisphenol A Derivatives as β-Amyloid Peptide Aggregation Inhibitors

Yu Zhou,[†,∞] Chunyi Jiang,[†,∞] Yaping Zhang,[∥,∞] Zhongjie Liang,[†] Wenfeng Liu,[†,⊥] Liefeng Wang,[#] Cheng Luo,[†] Tingting Zhong,[∥] Yi Sun,[∥] Linxiang Zhao,[⊥] Xin Xie,[†] Hualiang Jiang,[†] Naiming Zhou,*[,∥] Dongxiang Liu,*[,†] and Hong Liu*[,†]

[†]*State Key Laboratory of Drug Research, Shanghai Institute of Materia Medica, Chinese Academy of Sciences, Shanghai 201203, China,* [∥]*Institute of Biochemistry, College of Life Sciences, Zijingang Campus, Zhejiang University, Hangzhou, Zhejiang, 310058, China,* [⊥]*School of Pharmaceutical Engineering, Shenyang Pharmaceutical University, Shenyang, Liaoning 110016, China, and* [#]*Laboratory of Receptor-Based Bio-Medicine, School of Life Sciences and Technology, Tongji University, Shanghai 200092, China.* [∞]*These authors contributed equally to this work.*

Received January 15, 2010

The aggregation of Aβ is a crucial step in the etiology of Alzheimer's disease. Our previous work showed that Aβ undergoes α-helix/β-sheet intermediate structures during the conformational transition, and an Aβ aggregation inhibitor (**1**) was discovered by targeting the intermediates. Here, structure optimization toward compound **1** was performed and 34 novel derivatives were designed and synthesized. Nine compounds showed more effective inhibitory activity than the hit compound **1** in ThT fluorescence assay. Among them, compound **43** demonstrated more excellent inhibitory potency, which not only can suppress the aggregation of Aβ but also can dissolve the preformed fibrils as shown by CD spectroscopy, PICUP and AFM assays. Cellular assay indicated that **43** has no toxicity to neuronal cells, moreover, can effectively inhibit $A\beta_{1-42}$-induced neutrotoxicity and increase the cell viability. Together, on the basis of these positive results, these novel chemical structures may provide a promising potential for therapeutic applications in AD and other types of neurodegenerative disorders.

1. Introduction

Alzheimer's disease (AD[a]), the most common form of dementia in the elderly, is characterized by extracellular amyloid plaques and intraneuronal fibrillary tangles in the brain.[1−6] The growing number of AD patients due to increased life expectancy imposes a heavy financial burden on society.[7] Despite intensive studies, its molecular etiology is still enigmatic. A variety of drug treatments have been shown to benefit patients, but none of them represent a real cure.[8]

$A\beta_{1-40}$ and $A\beta_{1-42}$ are the main alloforms of β-amyloid (Aβ) peptides found in the amyloid plaques, which are generated by sequential action of β- and γ-secretase on the Aβ precursor protein (APP).[9] Although the amount of secreted $A\beta_{1-42}$ is only 10% of $A\beta_{1-40}$, $A\beta_{1-42}$ is the predominant component of AD plaques and displays an enhanced neurotoxicity relative to that of $A\beta_{1-40}$.[10−13] Several mechanisms have been proposed to explain the precise nature of the neuronal toxicity of Aβ peptides, but the cytotoxic mechanisms of Aβ has not been fully understood.[4] However, compelling evidence demonstrated that the soluble oligomers (amyloid-derived diffusible ligands, ADDLs) and fibrils of Aβ are the toxic components that cause neuronal injury and death in AD.[4,14] Therefore, chemicals that prevent the pathological oligomerization and fibrillation of Aβ have potential therapeutic applications in the treatment of AD.[15]

So far, many compounds have been found to block Aβ aggregation or neurotoxicity in vitro, including peptidic inhibitors and nonpeptidic small molecule inhibitors of Aβ aggregation.[16−18] However, the usefulness of these compounds as inhibitors against Aβ aggregation is often compromised by their lack of specificity and/or unknown mechanism of action and by the fact that many are toxic as well as have poor bioavailability in vivo.[19−21] Most of these compounds are so hydrophilic that they are unable to go across the blood−brain barrier (BBB).[4,19] Accordingly, both the structural modification of inhibitors and the design of new inhibitors with alternative structural scaffolds are required to improve the physiochemical properties.

Previously, we had studied the conformational transition of $A\beta_{1-40}$ from an α-helix to a random coil by using long-time molecular dynamics (MD) simulations.[22] The results showed that Aβ undergoes α-helix/β-sheet intermediate structures during the conformational transition. These α-helix/β-sheet intermediate structures have a core domain constituted by residues 24−37, of which four glycine residues (Gly25, Gly29, Gly33, and Gly37) are essential to the β-sheet formation and amyloid fibrillation. Virtual screening based on molecular docking was performed by targeting the C-terminal core region of the above Aβ intermediate structures, and a new inhibitor (DC-AB1, **1**, Scheme 1) was discovered.[4] Here, we continued to explore this class of compounds in order to optimize the structural

*To whom correspondence should be addressed. For N.Z.: phone, +86-21-571-88206748; fax, +86-571-88206485; e-mail, znm2000@yahoo.com. For D.L.: phone, +86-21-50806600-2302; fax, +86-21-50807088; e-mail, dxl@mail.shcnc.ac.cn. For H.L.: phone, +86-21-50807042; fax, +86-21-50807042; e-mail, hliu@mail.shcnc.ac.cn.

[a] Abbreviations: AD, Alzheimer's disease; Aβ, β-amyloid; APP, amyloid precursor protein; ADDLs, amyloid-derived diffusible ligands; MD, molecular dynamics; ThT, thioflavin T; CD, circular dichroism; PICUP, photoinduced cross-linking of unmodified proteins; AFM, atomic force microscopy.

Published on Web 07/21/2010

Scheme 1. Chemical Structure of Hit Compound **1**

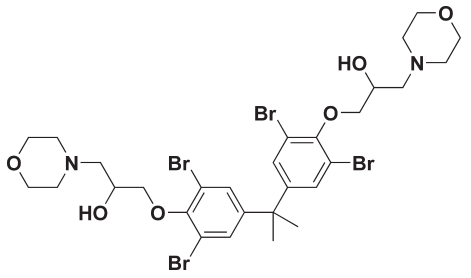

1 (DC-AB1)

features and to discover more potent derivatives with high efficacy. Thirty-four new compounds (**22**−**55**) have been designed, synthesized, and tested with various biological assays. Nine compounds have much higher potencies than the parental compound **1** in the thioflavin T (ThT) fluorescence assay. Among them, compound **43** demonstrated more efficient inhibitory activity against Aβ aggregation. Circular dichroism (CD) spectroscopy displayed that the β-sheet component of Aβ is increased in the presence of compound **43**, suggesting that **43** can stabilize its β-sheet conformation and further inhibit fibrillation of Aβ. In addition, compound **43** not only can dramatically suppress the oligomerization and fibrillation of Aβ but also was able to dissolve the preformed fibrils as shown by photoinduced cross-linking of unmodified proteins (PICUP) and atomic force microscopy (AFM) assays, respectively. Cellular assay for compound **43** indicated that **43** has nontoxicity to neuronal cells at and/or below 1 μM and can effectively inhibit Aβ_{1-42}-induced neutrotoxicity, increase the cell viability under certain concentrations.

2. Materials and Methods

2.1. Chemistry. 2.1.1. Design of Analogues of Compound 1. On the basis of the structural features of our reported compound **1** and the analysis toward the α-helix/β-sheet intermediate structure generated by MD simulations as well as the docking studies,[4,22] 34 new analogues (**22**−**55**) were designed and synthesized. According to the complex model of the parental compound **1** with Aβ_{1-40} generated by docking,[4] we found that the peptide surface was mainly constituted by some C-terminal residues Phe19, Phe20, Val24, Gly25, Gly29, Ala30, Gly33, Leu34, Gly38, Val39, and Val40 as well as a few N-terminal residues Ala2, Glu3, Arg5, Tyr10. Compound **1** binds to the C-terminal region mainly through hydrophobic interactions, and three major hydrophobic sites could be observed at the Aβ_{1-40} surface that hold the hydrophobic chemical groups of the model compound **1**. Two phenyl rings of **1** interact with two hydrophobic sites consisting of residues of Tyr10, Phe19, Phe20 (site A) and residues of Val24, Gly29, Val40 (site B), respectively. In addition, the morpholine segments of hit compound **1** interact with the third hydrophobic site constituted by residues of Leu34 and Val40 (site C). Consequently, hydrophobic interactions seem to be an important factor to keep the inhibitory activities against Aβ aggregation. According to these results, we tried to keep the hydrophobic interactions between target molecules and the Aβ surface in the design of new molecules. First, by replacing the terminal morpholine group of the hit compound **1** with a simple isostere of the morpholino ring, that is, the *N*-methylpiperizino ring, we obtained the target compound **22**. Then, we substituted all or part of the Br atoms with methyl substituents and/or H atoms and got the corresponding compounds **23**−**27**. Meanwhile, we introduced a piperidino ring instead of the *N*-methylpiperizino ring of compound **27** to form its derivative **28**. Subsequently, we investigated the linker propane-2,2-diyl moiety of target compounds and designed compounds **29**−**42** by substitution of the linker with other hydrophobic linkers, such as perfluoropropane-2,2-diyl, ethane-1,1-diyl, cyclopentane-1,1-diyl, cyclohexane-1,1-diyl, and cycloheptane-1,1-diyl moiety, respectively. In addition, basing on the complex model of the hit compound **1** and our previous research,[4] we further investigated the influences of various R_3 groups on the inhibitory activities against Aβ aggregation, such as introducing more flexible or rigid hydrophobic segments into the R_3 groups, and designed target compounds **43**−**55**.

2.1.2. Synthetic Procedures of Target Compounds. As shown in Scheme 2, compounds **1**, **22**, **25**−**28**, and **43**−**46** were first prepared by starting from commercially available bisphenol A analogues **1a**−**c**, which were first reacted with epichlorohydrin in the presence of KOH and phase-transfer-catalyst $Bu_4N^+Br^-$ to give intermediates **2a**−**c** and then treated with the corresponding amines in methanol as a solvent, respectively. On the other hand, some biphenols (**4**, **14**, and **17a**−**c**) were synthesized by treatment of phenols (**3** and **13**) with the corresponding ketones in the mixed solution of concentrated sulfuric acid and acetic acid, respectively. Treatment of biphenol **4** with epichlorohydrin could easily give the intermediate product **5**, which was further converted to the expected products **23**−**24** and **47**−**55** by treatment of the intermediate **5** with the corresponding amines in good yields, respectively. By bromination of 4,4′-(perfluoropropane-2,2-diyl)diphenol (**6**), an intermediate biphenol **7** was prepared, and further converted to another intermediate **8** by reacting with epichlorohydrin in the presence of KOH and $Bu_4N^+Br^-$. Then, by treatment of intermediate **8** with morpholine and *N*-methylpiperazine, compounds **29** and **30** were obtained with good yields, respectively. In addition, direct treatment of **6** with epichlorohydrin could give intermediate **9**, which was further converted into products **31** and **32** according to the synthetic procedure of **29** and **30**. The target product **33** can be also easily obtained from the starting material 4,4′-(ethane-1,1-diyl)-diphenol (**10**) by the synthetic procedure similar to that of **30**. Besides, compounds **34** and **35** were prepared by starting from phenol (**13**), which was first reacted with cyclopentanone to give an intermediate **14**, followed by bromination with Br_2 in acetic acid to give a biphenol intermediate **15**, which was further converted into intermediate **16** and then treated with morpholine and *N*-methylpiperazine to prepare the target compounds, respectively. With a similar synthetic procedure of **23**, we treated 2,6-dimethylphenol (**3**) with the corresponding cyclic ketones in concentrated sulfuric acid and acetic acid to give intermediates **17a**−**c**, respectively, which further converted to **18a**−**c** under the conditions of KOH and $Bu_4N^+Br^-$. Subsequently, by reaction of **18a**−**c** with the corresponding amines, compounds **36**−**39** and **41**−**42** were easily afforded. The target product **40** was synthesized from the starting material 4,4′-(cyclohexane-1,1-diyl)diphenol (**19**). First, bromation of compound **19** with 2 equiv of bromine gave intermediate **20**, which was further treated by epichlorohydrin to afford another intermediate **21**, which was followed by reacting with *N*-methylpiperazine to give product **40**.

Scheme 2[a]

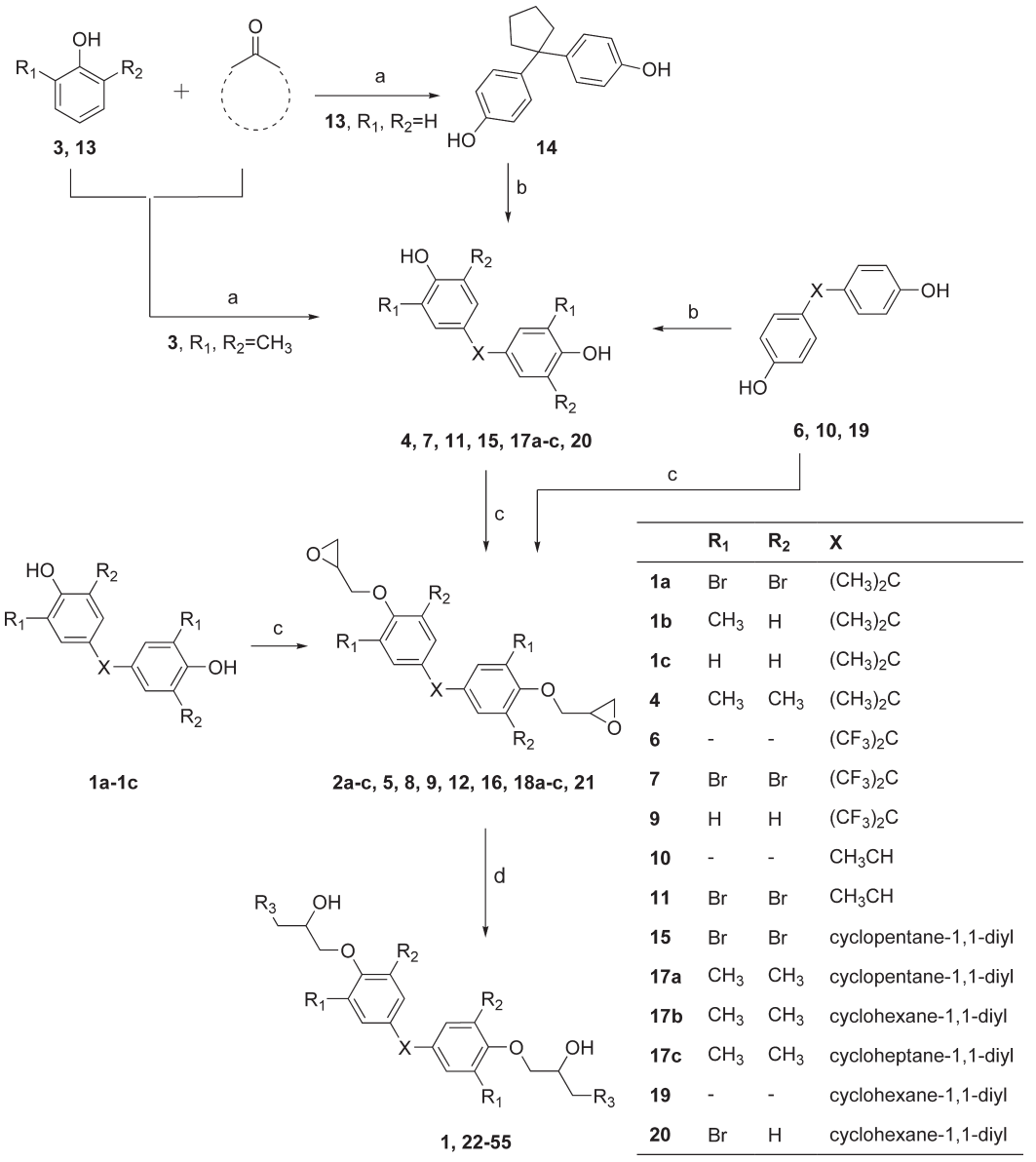

	R_1	R_2	X
1a	Br	Br	$(CH_3)_2C$
1b	CH_3	H	$(CH_3)_2C$
1c	H	H	$(CH_3)_2C$
4	CH_3	CH_3	$(CH_3)_2C$
6	-	-	$(CF_3)_2C$
7	Br	Br	$(CF_3)_2C$
9	H	H	$(CF_3)_2C$
10	-	-	CH_3CH
11	Br	Br	CH_3CH
15	Br	Br	cyclopentane-1,1-diyl
17a	CH_3	CH_3	cyclopentane-1,1-diyl
17b	CH_3	CH_3	cyclohexane-1,1-diyl
17c	CH_3	CH_3	cycloheptane-1,1-diyl
19	-	-	cyclohexane-1,1-diyl
20	Br	H	cyclohexane-1,1-diyl

[a] Reagents and conditions: (a) H_2SO_4 (2 equiv), AcOH, 15 °C, 1.5 h; (b) Br_2 (4 equiv), AcOH, room temp, 12 h; (c) KOH (4 equiv), $Bu_4N^+Br^-$ (0.2 equiv), epichlorohydrin, room temp, 12 h; (d) amines (2.2 equiv), CH_3OH, reflux, 3 h.

2.2. Biological Evaluation. 2.2.1. Thioflavin T (ThT) Fluorescence Assay. A screening assay for all compounds that inhibit $A\beta_{1-42}$ fibrillation was performed by measuring ThT fluorescence emission with a modified procedure described by Lee et al.[23]Amounts of 2 μL of compound (in concentrations of 0.1−10.0 mM) and 4 μL of 50 μM $A\beta_{1-42}$ were added into 64 μL of phosphate-buffered saline (PBS at pH 7.4, with 11% ethanol) in a 96-well plate. After incubation for 2 h at room temperature, 10 μL of 40 μM ThT solution (in PBS at pH 7.4, with 10% ethanol) was added to the reaction solution. Fluorescence was measured at 488 nm with an excitation wavelength of 430 nm on a multilevel HTS counter POLAR star OPTIMA (BMG LABTECH).

2.2.2. Circular Dichroism (CD) Spectroscopy Assay. A sample of 1,1,1,3,3,3-hexafluoroisopropanol (HFIP) treated $A\beta_{12-28}$ was dissolved in 50% (V/V) of 2,2,2-trifluoroethanol (TFE)/water and diluted to 80 μM. CD spectra were collected in a 0.1 cm path-length cuvette on a Jasco J-810 spectropolarimeter (JASCO Corporation, Japan). The data are the average of four scans over a wavelength of 190−260 nm at room temperature. The background signal from 50% TFE/water was subtracted. Deconvolution of CD spectra was performed with the software SOMCD (http://geneura.ugr.es/cgi-bin/somcd/index.cgi).

2.2.3. Photoinduced Cross-Linking of Unmodified Proteins (PICUP) Assay. $A\beta_{1-42}$ was first dissolved in HFIP and sonificated for 30 min to disassemble the pre-existing $A\beta_{1-42}$ aggregates and then dried over nitrogen. The sample was dissolved in Millipore water and used immediately for PICUP experiments. A 150 W xenon lamp was used as the irradiation source, and the exposure time was controlled by a timed switch. The reaction tube was positioned parallel to the beam of light at a distance of 10 cm from the lamp. Ammonium persulfate (APS, 200 mM) and 5 mM $Ru(bpy)_3Cl_2$ were added into the reaction tube sequentially according to the ratio $A\beta_{1-42}/Ru(bpy)_3Cl_2/APS = 1/4/80$. In all experiments, the samples were irradiated for 3 s. After irradiation, samples were immediately quenched with an

equal volume of loading buffer (0.1 M Tris/4% SDS/0.2 M DL-dithiothreitol/20% glycerol/0.001% bromophenol blue). Finally, the samples were heated at 95 °C for 5 min and separated by electrophoresis on a 15% tricine SDS−polyacrylamide gel.

2.2.4. Atomic Force Microscopy (AFM) Assay. $A\beta_{1-42}$ (200 μM, 5 μL), Millipore water (10 μL), and 10 mM **43** (5 μL) were incubated for 17 days at 37 °C. As a control, 200 μM $A\beta_{1-42}$ (10 μL), Millipore water (20 μL), and DMSO (10 μL) were incubated for 17 days at 37 °C. AFM experiments were performed as follows: the samples diluted 5 times with Millipore water were dropped on mica and then were blown dry.

$A\beta_{1-42}$ (200 μM, 10 μL) in Millipore water (20 μL) and DMSO (10 μL) was incubated for 17 days at 37 °C to form fibrils. Then 10 μL of the fibrils and 10 mM **43** (2.5 μL) were incubated together for 27 days at 37 °C, and 10 μL of the fibrils and 2.5 μL of DMSO were incubated for 27 days at 37 °C as a control. All samples were scanned under a Nanoscope IIIa atomic force microscope (Veeco Instruments Ltd.) with tapping mode.

2.2.5. Cell Assay. Differentiated rat pheochromocytoma (PC-12) cells were maintained in Dulbecco's modified Eagles medium (DMEM, Invitrogen) supplemented with 10% heat-inactivated fetal bovine serum (FBS, Hyclone) and 2 mM L-glutamine (Invitrogen) at 37 °C in an atmosphere of 5% CO_2. For cell viability assays, cells were trypsinized using 0.25% trypsin in Hank's solution containing 0.02% EDTA and plated in 96-well plates at a density of 10 000 cells per well in 100 μL of cell culture media. Experiments were performed 24 h after cells were seeded.

2.2.5.1. Primary Murine Neuronal Cell Cultures. Primary neuronal cultures of the cerebral cortex were prepared from postnatal ICR mice (PD 0-1) as described previously[24] with minor modifications. Briefly, the cerebral cortex was isolated and incubated for 20 min at 37 °C in Ca^{2+}, Mg^{2+}-free Hanks' balanced salt solution containing 0.25% trypsin (Sigma). Thereafter, the tissue was lightly triturated with a sterile Pasteur pipet followed by trituration with a fire-polished Pasteur pipet until no visible lumps of tissue remained. The cells were rinsed three times with PBS and resuspended in Neurobasal medium (Gibco) with B-27 supplement (Gibco), 0.5 mM L-glutamine, 50 IU/mL penicillin, and 50 μg/mL streptomycin (Gibco). After viable cells were counted, the cells were diluted with culture medium and seeded into poly-L-lysine-coated 96-well plate culture dishes at a density of 4×10^5 cells/mL. The neurons were cultured at 37 °C in an atmosphere of 5% CO_2 and 100% humidity. One-half of the medium was removed every 3 days and replaced with fresh medium to adjust to the original volume. The neurons were used for experiments after 8−9 days incubation. The animal experiments were approved by the Institutional Animal Care and Use Committee at Zhejiang University, China.

2.2.5.2. Preparation of Sample Solution. $A\beta_{1-42}$ was dissolved in sterile water containing 5% dimethyl sulfoxide (DMSO) to make a 50 μM stock solution. Mature fibrillars $A\beta_{1-42}$ were obtained by maintaining the $A\beta_{1-42}$ stock solution for 3 days at 37 °C. Compound **43** was dissolved completely in dimethyl sulfoxide (DMSO) to 100 mM. Small aliquots were stored at 4 °C before use.

2.2.5.3. Evaluation of the Compound and $A\beta_{1-42}$ Toxicity. To test for self-toxicity, the stock solution of the compound **43** was diluted in cell culture medium and then added to differentiated PC-12 cells at the desired concentrations of 0.1 nM to 100 μM. The $A\beta_{1-42}$ solution was prepared by diluting the stock solution into cell culture medium to yield concentrations of 1, 5, 10, 20, and 50 μM ($A\beta_{1-42}$) and incubated for 48 h. Negative controls included DMSO at the same concentration as in the compound solutions and media alone. The positive control was 5 μM staurosporine to induce complete cell death. The staurosporine control was used to establish the dynamic range of the experiment and represented a 100% reduction in cell viability, upon which the percentage viability of all the experimental conditions was calculated. Cell viability was assessed qualitatively by visual observation and quantitatively by the CellTiter 96 nonradioactive cell proliferation assay (Promega). In brief, 15 μL of dye solution was incubated with the cells for 4 h. Then 100 μL of solubilization/stop solution was added and the plates were incubated overnight to ensure complete solubilization. Plates were read by using the ELX800 universal microplate reader (BioTek), and the absorbance at 570 nm (formazan product) was recorded. Corrected absorbance was used to calculate the percent cell viability from the experimental change (Amedia-Aexperimental) over the dynamic range (Amedia-Astaurosporine). At least three independent experiments with three replicates ($n \geq 9$) were carried out, and the results were averaged.

2.2.5.4. Evaluation of the Compound for Inhibition of $A\beta_{1-42}$-Induced Neurotoxicity. To test compound **43** for the ability to inhibit $A\beta_{1-42}$-induced toxicity, $A\beta_{1-42}$ solution and compound **43** were prepared; the stock solution of the compound **43** was diluted with $A\beta_{1-42}$ solution. The mixtures were added to cells to yield final concentrations of 0, 0.01, 0.1, 0.3, 1, and 3 μM (compound **43**) and 10 μM $A\beta_{1-42}$. Cell viability was determined by the MTT assay as described above. At least three independent experiments with three replicates ($n \geq 9$) were carried out, and the results were averaged. The compound that showed strong inhibition of $A\beta_{1-42}$-induced toxicity was studied further to determine their dose-dependent activity. Dose-dependence MTT experiments were conducted as described above with 0, 0.003, 0.03, 0.3, and 3 μM (compound **43**) and 10 μM $A\beta_{1-42}$. Three independent experiments with three replicates ($n \geq 9$) were carried out, and results were averaged.

2.2.6. γ-Secretase Fluorogenic Substrate Assay. An amount of 10 μg of membrane protein was added to each well of a 96-well plate with 6 μM fluorogenic substrate. Compounds were added at the indicated concentrations, and the final reaction system was adjusted to 100 μL/well with the reaction buffer. The plate was incubated at 37 °C in a humidified atmosphere for 5 h. Fluorescence was measured using a BIOTEK FLX800 microplate reader with the excitation wavelength at 355 nm and the emission wavelength at 440 nm. The γ-secretase inhibitor L685,458 was used as the positive control. Data were analyzed with GraphPad Prism software (GraphPad, San Diego, CA). Nonlinear regression analyses were performed to generate dose-response curves and calculate IC_{50} values.

2.3. Molecular Modeling. The 3D structure of $A\beta$ in complex with the inhibitor **1** was retrieved from our previous study.[4] First, the ligand was removed and polar hydrogen atoms were added. Then the potential of the 3D structure of $A\beta$ was assigned with Kollman-united-atom[25] charges encoded in the SYBYL molecular simulation package. The molecular geometries of all small molecules were also modeled using SYBYL assigned with Gasteiger−Huckel charges. The initial structures were minimized using molecular mechanics

with the Tripos force field with the current charges, and the energy convergence gradient value was set to 0.05 kcal/(mol·Å). To determine the binding mode of these inhibitors to Aβ, the docking program AutoDock 3.0.3[26] was used to automatically dock the inhibitors to the enzyme. The Lamarckian genetic algorithm (LGA) was applied to deal with the protein−inhibitor interactions. A Solis and Wets local search was performed for energy minimization on a user-specified proportion of the population. The docked structures of the inhibitors were generated after a reasonable number of evaluations. The whole procedure of docking simulation in this study could be stated as follows. First, the Aβ structure was checked for polar hydrogens and assigned partial atomic charges, and a PDBQ file was created. Atomic solvation parameters and fragmental volumes were assigned to Aβ using the ADDSOL module of the AutoDock program. Meanwhile, some of the torsion angles of the inhibitors were defined, allowing a conformational search for the ligands during the docking process. Second, the grid map with $80 \times 80 \times 80$ points and a spacing of 0.375 Å was calculated using the Autogrid program to evaluate the binding energies between the inhibitors and the protease. The grid center was set at the active site position (43.566, 36.747, 37.807), and the affinity and electrostatic potential grids were calculated for each type of atom in the inhibitors. The energetic configuration of a particular inhibitor was found by trilinear interpolation of affinity values and electrostatic interaction of the eight grid points around each atom of the inhibitor. Third, some important parameters for LGA calculations were reasonably set up according to requirements of the Amber force field and our problem. The starting position and conformation was set as random, and the initial number of individuals in the population was 50. The step size was set to 0.2 Å for translation and 5° for orientation and torsion. The maximum numbers of generations, energy evaluations, and docking runs were set to 2.7×10^4, 1.5×10^6, and 20, respectively. The elitism value was 1, which automatically survived into the next generation. The mutation rate was 0.02, which is the probability that a gene would undergo a random change. The crossover rate, the probability of proportional selection, was 0.80. The pseudo Solis and Wets local search method with a maximum of 300 iterations per local search was used. The probability of performing local search of an individual in the population was 0.06. The maximum number of consecutive successes before doubling or halving the local search step size was 4 and was the same as the number of failures. The lower bound on *F*, the termination criterion for the local search, was 0.01. Twenty docking simulations were performed for each inhibitor, and conformations of multiple runs were then clustered with the root-mean-square deviation (rmsd) tolerance of 1.0 Å. Finally, the proper conformation and position compared with the complex structure were extracted from the optimized complex.

3. Results and Discussion

3.1. Chemistry. On the basis of the structural features of hit compound **1** as well as its docking simulation toward Aβ extracted from the trajectory of MD simulations on Aβ_{1-40}, 34 new compounds were designed and synthesized, and their chemical structures (**22**−**55**) are shown in Table 1. These target compounds were synthesized according to the routes outlined in Scheme 2. The details of the synthetic procedures and structural characterizations are described in the Experimental Section.

3.2. Biological Evaluation. 3.2.1. Structure−Activity Relationship Regarding Inhibition of Aβ Aggregation. All substances were evaluated for their inhibitory activities against Aβ aggregation by the ThT assay. ThT exhibits a characteristic fluorescence spectral change upon binding to amyloid fibrils. The maximum emission wavelength was shifted from 445 to 482 nm.[4,27] The more fibrils it binds, the stronger fluorescence intensity will be. As shown in Table 1, nine of the synthesized analogues (**40**, **43**−**45**, **47**, and **50**−**53**) demonstrated more effective inhibitory potency against Aβ aggregation than the parental compound **1** ($IC_{50} = 26\ \mu M$),[4] with the IC_{50} values ranging from 0.27 μM (**45**) to 13 μM (**40**), and five compounds (**22**, **30**, **33**, **35**, and **48**) displayed an equivalent inhibitory potency against Aβ aggregation to the hit compound. According to these results, a similar inhibitory activity against Aβ aggregation was observed when replacing the morpholino moiety of the parental compound **1** with a simple isostere *N*-methylpiperizino segment, which indicates that this slight modification does not have a remarkable influence on the inhibitory potency. However, when four Br atoms of hit compound **1** were replaced by CH_3 substituents, the inhibitory potency of the resulting compound **23** was dramatically decreased compared with the hit compound **1**. Therefore, further structural modifications for **23** were essential, and when we substituted the morpholino groups of **23** with the *N*-methylpiperazino groups, unfortunately, no better inhibitory activity was detected (**24**). Additionally, no improvement in inhibitory activities was observed when four Br atoms of the hit compound **1** and its derivatives were substituted by two CH_3 units and two hydrogen atoms or four hydrogen atoms to form **25**−**27**. However, when introducing a piperidino ring into the corresponding position of compound **26** to form compound **28**, a slight improvement of inhibitory activity against Aβ aggregation was detected. In order to explore the influence of linker (propane-2,2-diyl moiety) of the hit compound **1** on the inhibitory activities against Aβ aggregation, compounds **29**−**42** were synthesized by substitution of the linker of **1** with other hydrophobic linkers, such as perfluoropropane-2,2-diyl, ethane-1,1-diyl, cyclopentane-1,1-diyl, cyclohexane-1,1-diyl, and cycloheptane-1,1-diyl moieties, respectively. Although compound **30** showed the most potent activity among compounds **29**−**32**, which were obtained by replacement of the linker $(CH_3)_2C$ unit of **1** with a $(CF_3)_2C$ unit, no significant improvement of the inhibitory potency against Aβ aggregation compared to **1** was detected. However, substitution of the linker of compound **22** with CH_3CH moiety to give compound **33** has an equivalent inhibitory potency against Aβ aggregation compared to hit **1**. To further optimize the linkers of molecular structures, cyclopentane-1,1-diyl, cyclohexane-1,1-diyl, and cycloheptane-1,1-diyl were introduced into the linker positions of **1** and **22**−**24**, respectively. Unfortunately, no better results were achieved (**34**−**39** and **41**, **42**). However, replacement of four methyl moieties of compound **39** with two hydrogen atoms and two bromo atoms to give compound **40** resulted in a slight enhancement of inhibitory potency against Aβ aggregation. Subsequently, in order to improve the inhibitory activities against Aβ aggregation, we further investigated the influences of various R_3 groups on the inhibitory activities, involving the introduction of some more flexible or rigid hydrophobic segments into the R_3 groups. Excitingly, a significant improvement in the inhibitory activities against Aβ aggregation was observed when replacing the morpholino moiety of the

Table 1. Structures of Target Compounds and Their Aβ Aggregation Inhibitory Activities by ThT Bioassay

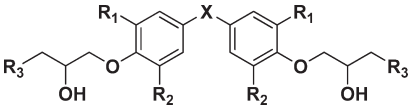

Compound	X	R_1	R_2	R_3	IC_{50} (μM)
1	$(CH_3)_2C$	Br	Br		26
22	$(CH_3)_2C$	Br	Br		23
23	$(CH_3)_2C$	CH_3	CH_3		N/A
24	$(CH_3)_2C$	CH_3	CH_3		N/A
25	$(CH_3)_2C$	CH_3	H		N/A
26	$(CH_3)_2C$	H	H		N/A
27	$(CH_3)_2C$	H	H		N/A
28	$(CH_3)_2C$	H	H		110
29	$(CF_3)_2C$	Br	Br		N/A
30	$(CF_3)_2C$	Br	Br		24
31	$(CF_3)_2C$	H	H		N/A
32	$(CF_3)_2C$	H	H		380
33	CH_3CH	Br	Br		25
34		Br	Br		N/A
35		Br	Br		24
36		CH_3	CH_3		N/A
37		CH_3	CH_3		56
38		CH_3	CH_3		N/A

Table 1. Continued

Compound	X	R_1	R_2	R_3	IC_{50} (μM)
39		CH_3	CH_3		70
40		Br	H		13
41		CH_3	CH_3		N/A
42		CH_3	CH_3		32
43	$(CH_3)_2C$	Br	Br		4.8
44	$(CH_3)_2C$	Br	Br	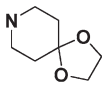	4.7
45	$(CH_3)_2C$	Br	Br	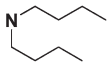	0.27
46	$(CH_3)_2C$	Br	Br	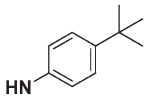	N/A
47	$(CH_3)_2C$	CH_3	CH_3		8.9
48	$(CH_3)_2C$	CH_3	CH_3	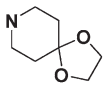	20
49	$(CH_3)_2C$	CH_3	CH_3		43
50	$(CH_3)_2C$	CH_3	CH_3		6.2
51	$(CH_3)_2C$	CH_3	CH_3		11
52	$(CH_3)_2C$	CH_3	CH_3	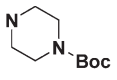	0.4
53	$(CH_3)_2C$	CH_3	CH_3	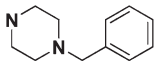	6.2
54	$(CH_3)_2C$	CH_3	CH_3	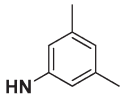	N/A
55	$(CH_3)_2C$	CH_3	CH_3	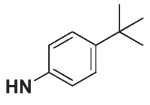	N/A

parental compound **1** with larger hydrophobic and/or more flexible groups. For example, introducing the 3,5-dimethylpiperidino group (**43**) and 1,4-dioxa-8-azaspiro[4.5]decan-8-yl group (**44**) into the position of the morpholino group of **1** gave a 5-fold improvement of the inhibitory potency against Aβ aggregation, respectively. A 100-fold improvement was observed by substitution of the morpholino group with a much more flexible dibutylamino moiety (**45**). However,

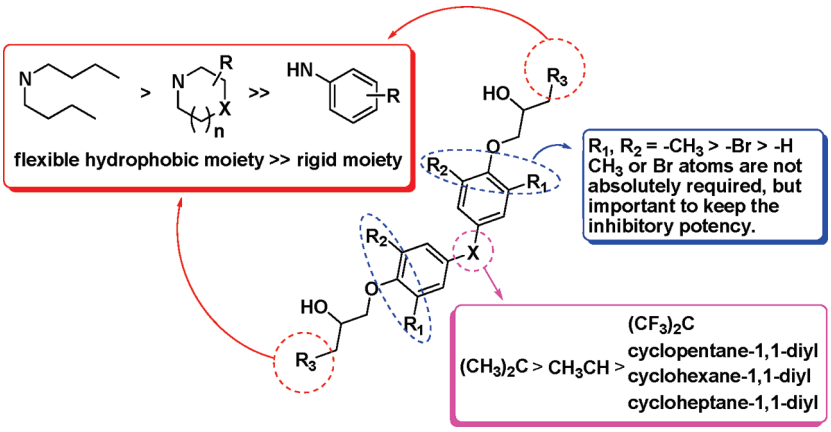

Figure 1. Schematic diagram of structure−activity relationships.

replacement of the morpholino groups with rigid aryl-ring moieties led to a dramatic loss of inhibitory activity against Aβ aggregation (**46**), indicating that a flexible substituent at the position of the R_3 group is important to the inhibitory potency against Aβ aggregation. On the basis of the above findings, we further replaced the morpholino moiety of compound **23** with some similar substituents as compounds **43**−**46**, and the results demonstrated that introducing some flexible hydrophobic moieties, such as the 3,5-dimethylpiperidino group (**47**), 1,4-dioxa-8-azaspiro[4.5]-decan-8-yl (**48**), piperidino group (**49**), azepan-1-yl (**50**), pyrrolidin-1-yl (**51**), *N*-boc-piperazino (**52**), or *N*-benzylpiperazino group (**53**), significantly improved the inhibitory potencies against Aβ aggregation compared to hit compound **1** except in the case of compound **49**. Among them, **52** is the most effective compound and has 60 times higher activity than hit compound **1**. These results indicate that Br atoms are not absolutely required but important to keep the inhibitory potency against Aβ aggregation. Substitution of the morpholino groups of **23** with different rigid aryl groups to give compounds **54** and **55** still resulted in the similar loss of inhibitory activities against Aβ aggregation, indicating that introduction of rigid aryl units into the R_3 position impaired the inhibitory potencies of target compounds against Aβ aggregation. The structure−activity relationships (SAR) are summarized in Figure 1.

3.2.2. CD Assay for Compound 43. It was reported that Aβ_{1-42} adopts a conformation mixture of α-helix, β-sheet, and random coil in aqueous solution and undergoes a conformational change to form intramolecular β-sheet structure in the fibrillation.[28] The conformational transition of the fragment of Val12-Lys28 into β-sheet was considered important for the amyloid formation.[29,30] Some Aβ_{1-42} inhibitors were proposed to bind to Val12-Lys28 of Aβ_{1-42}.[31] To investigate how compound **43** affects Aβ aggregation, we thus studied the conformational change of Aβ_{12-28} induced by compound **43** with CD spectroscopy (Figure 2). In 50% TFE, a polar solvent that can stabilize the α-helix and disrupt the interstrand hydrogen bond of β-sheet, Aβ_{12-28} displays a mixed conformation of α-helix, β-sheet, and random coil. The addition of compound **43** to Aβ_{12-28} induced a significant conformational change. The typical negative bands at 218 and 220 nm representing an α-helix decreased and a negative band at 216 nm was observed, indicating the appearance of a β-sheet conformation. According to the CD deconvolution results (Table 2), Aβ_{12-28} in 50% TFE adopted a conformational mixture containing 53.3% of α-helix, 16.3% of β-sheet, 6.2% of β-turn, and 24.1% of random coil. When **43** was added in

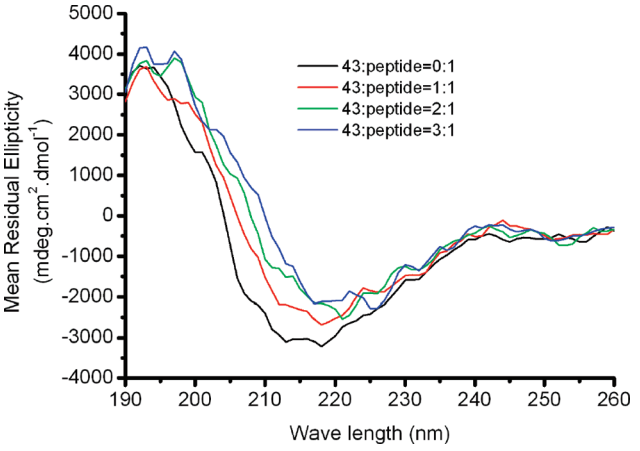

Figure 2. CD spectroscopy of Aβ_{12-28} with compound **43**. The CD spectra were recorded in a 0.1 cm path-length cuvette over a wavelength of 190−260 nm with a scan speed of 100 nm/s at room temperature. The data were the average of four time scans with an interval of 1 nm. The background signal from 50% TFE/water was subtracted.

Table 2. Deconvolution Results of Aβ_{12-28} CD Spectra[a]

	in 50% TFE			
	Aβ_{12-28}	Aβ_{12-28}/**43**[b]	Aβ_{12-28}/**43**[c]	Aβ_{12-28}/**43**[d]
helix	0.533	0.520	0.426	0.404
β-sheet[e]	0.163	0.175	0.171	0.174
β-turn	0.062	0.061	0.130	0.137
random coil	0.241	0.245	0.274	0.284

[a] The CD data were handled with software SOMCD (http://geneura.ugr.es/cgi-bin/somcd/index.cgi). [b] Aβ_{12-28} and **43** are in equimolar concentration. [c] Aβ_{12-28} and **43** are in ratio 1:2. [d] Aβ_{12-28} and **43** are in ratio 1:3. [e] Content of antiparallel β-sheet and parallel β-sheet conformations.

the ratio of 3:1 (compound **43**/Aβ_{12-28}), the β-sheet component was increased from 16.3% to 17.4% while the β-turn component was increased from 6.2% to 13.7% and the α-helix component was decreased from 53.3% to 40.4%, respectively. This suggests that some Aβ_{12-28} residues with α-helical conformation had been converted to β-sheet and β-turn conformation upon interaction with compound **43**. The binding of **43** increased the β-sheet content of Aβ peptide, probably because the binding of **43** at the C-terminal region of the intermediate structure of Aβ peptide might stabilize the β-sheet conformation of the monomeric peptide. The interaction between **43** and the C-terminal region shields the key residues at the C-terminus from interacting with the residues at the N-terminus,

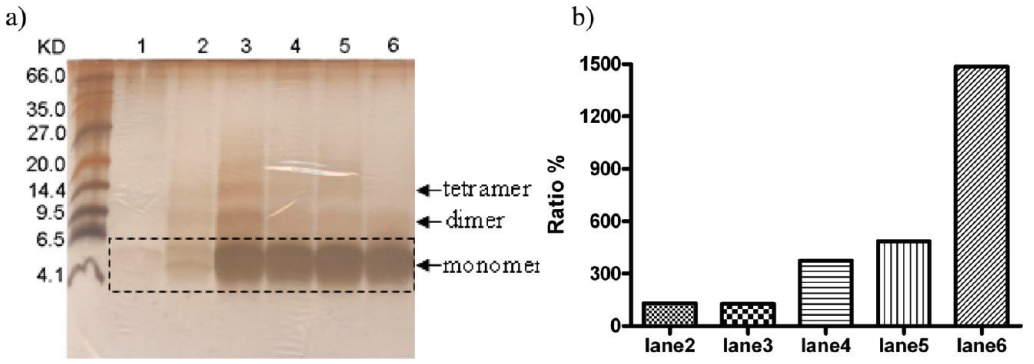

Figure 3. (a) Result of PICUP for confirming that compound **43** inhibits $A\beta_{1-42}$ aggregation: (lane 1) $A\beta_{1-42}$ (80 μM) incubated at 37 °C for 5 days in water bath; (lane 2) $A\beta_{1-42}$ (80 μM) at −80 °C for 5 days; (lane 3) $A\beta_{1-42}$ (80 μM) with **43** at −80 °C for 5 days; (lane 4) $A\beta_{1-42}$ (80 μM) with **43** incubated at 37 °C for 1 days in water bath; (lane 5) $A\beta_{1-42}$ (80 μM) with **43** incubated at 37 °C for 2 days in water bath; (lane 6) $A\beta_{1-42}$ (80 μM) with **43** incubated at 37 °C for 3 days in water bath. In all experiments, the ratio of $A\beta_{1-42}$/**43** was 1:10. (b) Ratio of (pixels of monomer)/(pixels of dimers + tetramers).

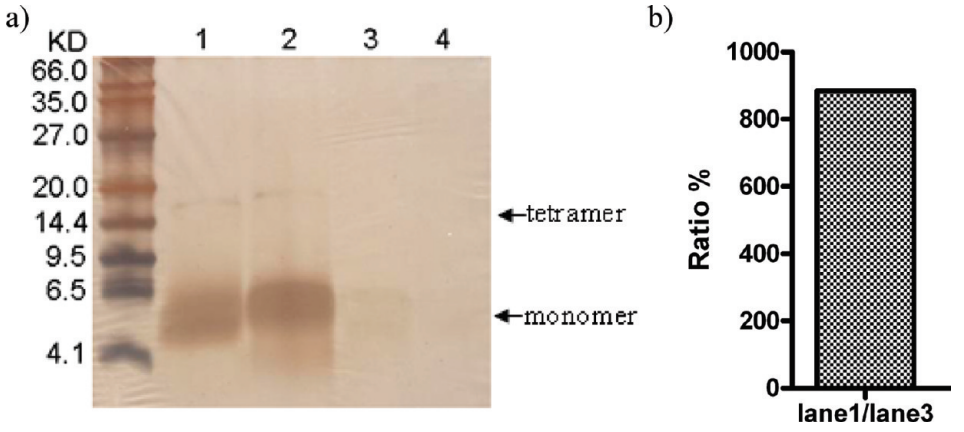

Figure 4. (a) Result of PICUP for confirming that compound **43** dissolves $A\beta_{1-42}$ fibrils: (lanes 1 and 2) $A\beta_{1-42}$ fibrils incubated with **43** at 37 °C for 18 days in water bath; (lanes 3 and 4) $A\beta_{1-42}$ fibrils not incubated with **43** at 37 °C for 18 days in water bath. In all experiments, the ratio of $A\beta_{1-42}$/**43** was 1:10. (b) Ratio of (pixels of monomer of lane 1)/(pixels of monomer of lane 3).

thereby interrupting Aβ to form antiparallel β-sheet structure that is a rate-determining step toward fibril formation, and further inhibits Aβ fibrillation.

3.2.3. PICUP Assay for Compound 43. $A\beta_{1-42}$ is prone to aggregate into oligomers and fibrils. PICUP assay had been used to study the oligomeric state of $A\beta_{1-42}$.[32] As shown in Figure 3a, a slight band near 4.1 kDa (lane 1), representing the monomer of $A\beta_{1-42}$, was observed for 80 μM $A\beta_{1-42}$ incubated at 37 °C for 5 days, which suggests that most of the monomeric $A\beta_{1-42}$ had aggregated into fibrils after incubation at 37 °C for 5 days. When $A\beta_{1-42}$ was incubated with compound **43** at 37 °C, there was an obvious thick band near 4.1 kDa (lane 4). It means that **43** can inhibit the aggregation of $A\beta_{1-42}$ to form fibrils. Meanwhile, the amount of $A\beta_{1-42}$ oligomers was decreased along with the incubation time at 37 °C (lanes 4−6 and Figure 3b). It was reported that storing Aβ peptides at −80 °C could slow the formation of fibrils.[33] We thus want to investigate whether **43** could inhibit fibrils formation more effectively than at −80 °C, and which temperature, 37 or −80 °C, is more beneficial for evaluating the inhibitory activity of **43** against fibril formation. Therefore, we stored the samples at −80 °C. As shown in Figure 3a (lanes 2 and 3), $A\beta_{1-42}$ stored at −80 °C without incubation with **43** for 5 days displayed several slight bands near 4.1, 9.5, and 14.4 kDa (lane 2), representing the monomer, dimer, and tetramer of $A\beta_{1-42}$, respectively. However, when compound **43** was added to $A\beta_{1-42}$ and kept at −80 °C for 5 days, $A\beta_{1-42}$ mainly kept its monomeric state and only a small proportion of $A\beta_{1-42}$ formed oligomers (lane 3). Comparing lane 2 and lane 3 with lane 4, respectively, we found that **43** could work better at 37 °C than at −80 °C. Besides, the PICUP assay also confirmed that compound **43** could dissolve the preformed $A\beta_{1-42}$ fibrils into monomers and a slight amount of oligomers, as shown in Figure 4. Therefore, it seems that compound **43** not only can inhibit $A\beta_{1-42}$ aggregation but also can effectively dissolve $A\beta_{1-42}$ fibrils.

3.2.4. AFM Assay for Compound 43. An amount of 50 μM $A\beta_{1-42}$ in 25% DMSO Millipore water was incubated at 37 °C for 17 days. AFM images demonstrated that $A\beta_{1-42}$ formed into fibrils and some small aggregates (Figure 5a). In contrast, no fibrils but some aggregates were detected when $A\beta_{1-42}$ was incubated with compound **43** (Figure 5b). Apparently, **43** had effectively inhibited the fibril formation of $A\beta_{1-42}$. Further, we incubated the preformed $A\beta_{1-42}$ fibrils (Figure 5c) with 2 mM **43** at 37 °C for 27 days. Obviously, compound **43** could effectively dissolve the $A\beta_{1-42}$ fibrils (Figure 5d), and only a little amount of aggregates was detected. However, as shown in Figure 3a, lanes 1 and 2, $A\beta_{1-42}$ was not incubated with compound **43** and we can also

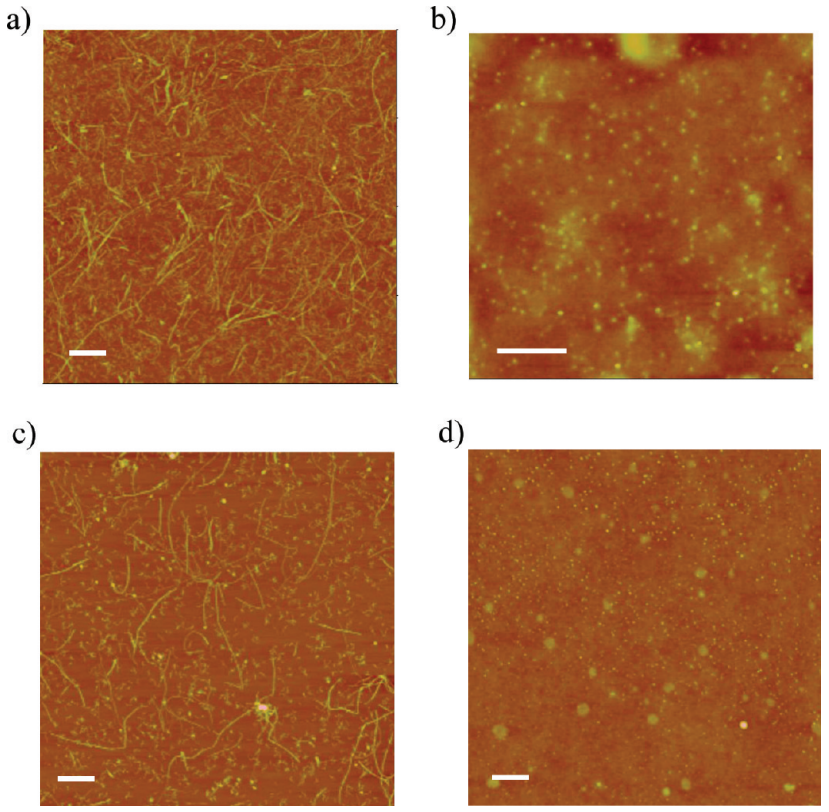

Figure 5. Morphological study of $A\beta_{1-42}$ fibrils by AFM experiment: (a) AFM scan image of 50 μM $A\beta_{1-42}$ incubated 17 days at 37 °C; (b) AFM scan image of a 50 μM $A\beta_{1-42}$ incubated with 2.5 mM **43** for 17 days at 37 °C; (c) AFM scan image of 50 μM $A\beta_{1-42}$ fibrils incubated with DMSO for 27 days at 37 °C; (d) AFM scan image of 50 μM $A\beta_{1-42}$ fibrils incubated with 2 mM **43** for 27 days at 37 °C. Scale bars are 1 μM.

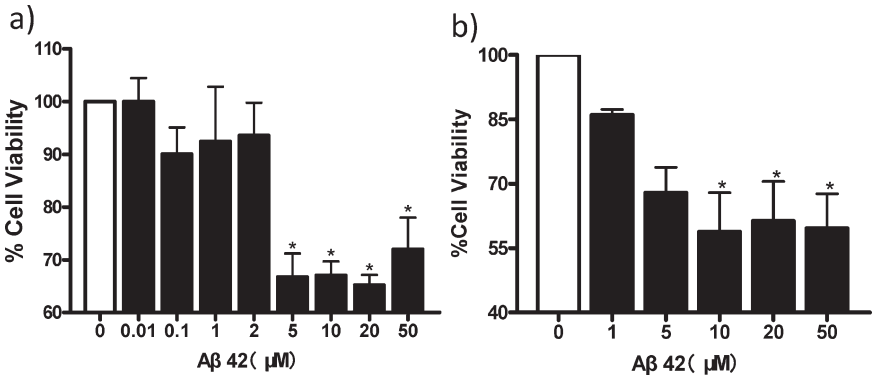

Figure 6. Neurotoxic effect of $A\beta_{1-42}$. Cells were exposed to various concentrations of $A\beta_{1-42}$. Cell viability was determined by MTT assay after 48 h: (a) neurotoxic effect of $A\beta_{1-42}$ on primary neuronal cells; (b) neurotoxic effect of $A\beta_{1-42}$ on differentiated PC-12 cells .Values are expressed as percentage of control values. Data are the mean ± SEM of two independent experiments with three replicates for each condition. Each treatment group was compared with the 0 groups using the Dunnett test after one-way ANOVA: (*) $p < 0.05$ when compared with the control group untreated $A\beta_{1-42}$.

detect a small amount of monomer, even dimer and tetramer, indicating that most of $A\beta_{1-42}$ peptides were assembled into fibrils and a small quantity of $A\beta_{1-42}$ peptide remained as monomer and/or aggregates. On the basis of these findings, the above-mentioned aggregates (Figure 5d) were formed by self-assembling of $A\beta_{1-42}$ peptides but not induced by compound **43**. Therefore, the results of the AFM assay are in accord with the results of the PICUP assay, both of which demonstrate that compound **43** is an effective inhibitor of $A\beta_{1-42}$.

3.2.5. Evaluation of the Compound 43 and $A\beta_{1-42}$ Toxicity. Treatment of primary cortical neurons with $A\beta_{1-42}$ decreased the number of viable cells in a dose dependent fashion. The decrease was statistically significant at a dose of 5 μM and higher (Figure 6a). For PC-12 cells, a concentration-dependent decrease of cell survival was also observed after exposure to $A\beta_{1-42}$ (Figure 6b). When cortical neurons were exposed to $A\beta_{1-42}$ for 48 h, 66.7 ± 8.9%, 67.0 ± 6.9%, and 65.2 ± 5.7% cell deaths were observed at 5, 10, and 20 μM $A\beta_{1-42}$, respectively. No cytotoxic effects were observed at and/or below 2 μM. Therefore, in the following experiments, 5 μM was selected to determine $A\beta_{1-42}$-induced neuronal cell damage in primary cortical neurons. A concentration of 10 μM was used for the determination of

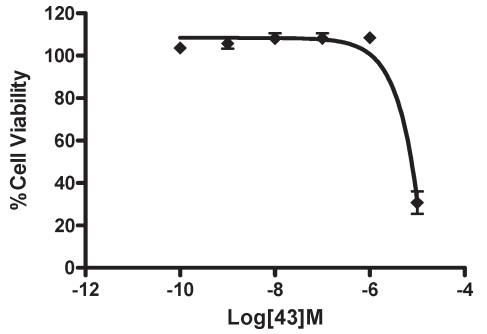

Figure 7. Evaluation of the effect of compound **43** on neuronal cultures. Cells were exposed to various concentrations of compound **43**. Cell viability was determined by MTT assay after 48 h. Values are expressed as percentage of control values. Data are the mean ± SEM of three independent experiments with three replicates for each condition.

$A\beta_{1-42}$-induced neurotoxicity on PC-12 cells. In contrast, compound **43** showed no toxicity to neuronal cells at and/or below 1 μM by the MTT cell-metabolism assay (Figure 7), suggesting that neuronal cells could be used for determining the inhibition of $A\beta_{1-42}$-induced toxicity.

3.2.6. Evaluation of Compound 43 for Inhibition of $A\beta_{1-42}$-Induced Neurotoxicity. PC-12 cells were treated with 10 μM $A\beta_{1-42}$ for 48 h in the absence or presence of different concentrations of compound **43**. The results demonstrated that in the presence of $A\beta_{1-42}$ (10 μM), treatment with compound **43** (10 μM) significantly increased the number of viable cortical neurons compared to those without compound **43** (Figure 8a). As shown in Figure 8b, for PC-12 cells, the assay showed that 1 and 3 μM **43** reversed the $A\beta_{1-42}$-induced (10 μM) neurotoxicity by 96.6 ± 6.2 and 104.2 ± 10.0%, respectively. To study the effectiveness of compound **43** as an inhibitor of $A\beta_{1-42}$-induced toxicity, a dose-dependent curve was generated. Compound **43** yielded IC_{50} values of 0.8 ± 0.4 μM in the MTT assay (Figure 8c). To examine the effects of **43** on the $A\beta_{1-42}$-induced morphological change and cytotoxicity, PC-12 cells were incubated with 10 μM $A\beta_{1-42}$, 10 μM $A\beta_{1-42}$ plus 3 μM **43**, or 0.02% DMSO for 48 h, respectively. As shown in Figure 9, MTT and microscopy observation indicated that DMSO treatment did not reveal any cytotoxic effects as expected while $A\beta_{1-42}$ treatment induced significant cell death. Incubation with 3 μM **43** resulted in a significant improvement in cell survival, suggesting that the aggregated $A\beta_{1-42}$ has a cytotoxic effect on PC-12 cells, and this compound can inhibit the toxicity and restore the cell number and the amount of MTT formazan.

3.2.7. γ-Secretase Fluorogenic Substrate Assay for 43, 45, and 52. It was reported that some bisphenol A derivatives could inhibit γ-secretase.[34] We selected the most effective compounds in relative assays for evaluating Aβ aggregation (**43**, **45**, and **52**) to measure their inhibitory activities against γ-secretase. Surprisingly, we found that compounds **43** and **52** showed good inhibitory effects against γ-secretase, and their values of IC_{50} were 5.57 and 1.82 μM, respectively. In view of these positive results, these compounds also provide a potential for the development of Aβ aggregation and γ-secretase dual inhibitors (see Supporting Information for details).

3.2.8. Binding Models. To explore structural information for further structural optimization, some representative compounds (**1**, **43**, **45**, and **52**) were selected for docking

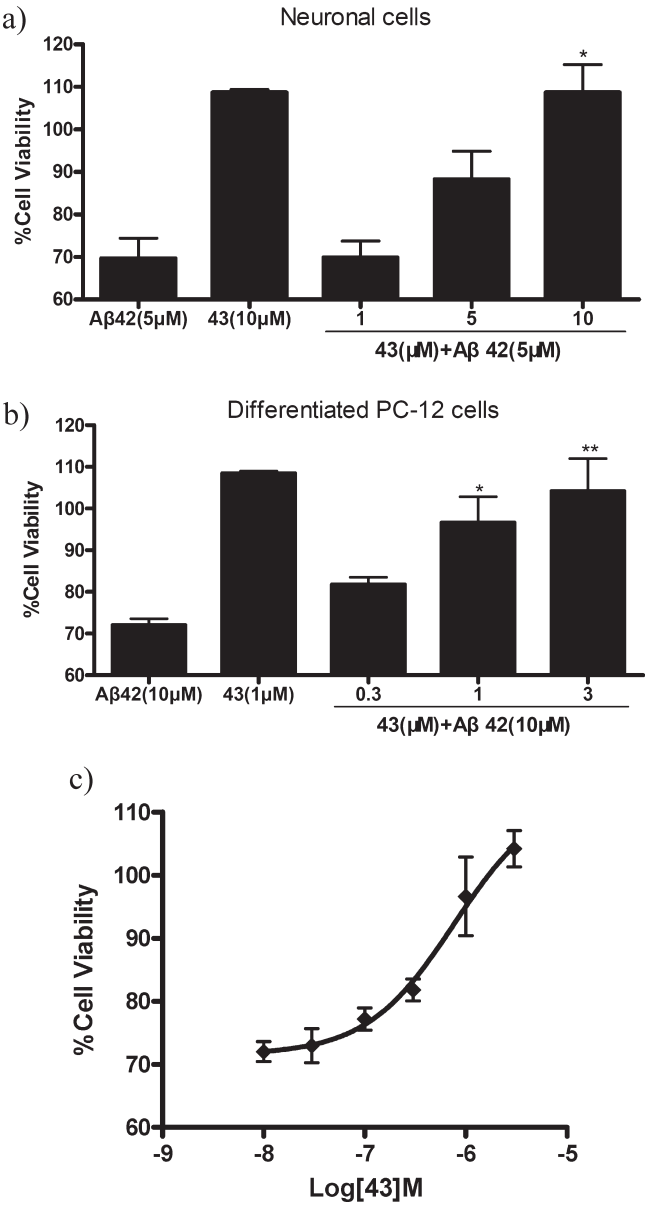

Figure 8. Evaluation of the compound **43** for inhibition of $A\beta_{1-42}$-induced neurotoxicity. Cell viability was determined by the MTT assay after 48 h: (a) inhibitory activity of the compound **43** on primary neuronal cells; (b) inhibitory activity of the compound **43** on differentiated PC-12 cells; (c) dose-dependent curve for the inhibition of **43** againt $A\beta_{1-42}$-induced toxicity on differentiated PC-12 cells. The data were normalized to full-kill and media controls and reported as the mean ± SEM of three independent experiments with three replicates for each condition. Each treatment group was compared with the $A\beta_{1-42}$ groups using the Dunnett test after one-way ANOVA: (*) $p < 0.05$ when compared with the control group treated only with 5 or 10 μM $A\beta_{1-42}$.

simulation studies. It is reported that Aβ peptides cleaved from the amyloid precursor protein (APP) usually adopt a conformational mixture of random coil, β-sheet, and α-helix in solution. By molecular dynamics simulation, we found that Aβ undergoes α-helix/β-sheet intermediate structures during the α-helix to random coil conformational transition and got the intermediate structure at 50 ns.[22] Molecular docking was performed by targeting this Aβ intermediate structure, and the result indicated that in a manner similar to the binding model of the hit compound **1**, the complex

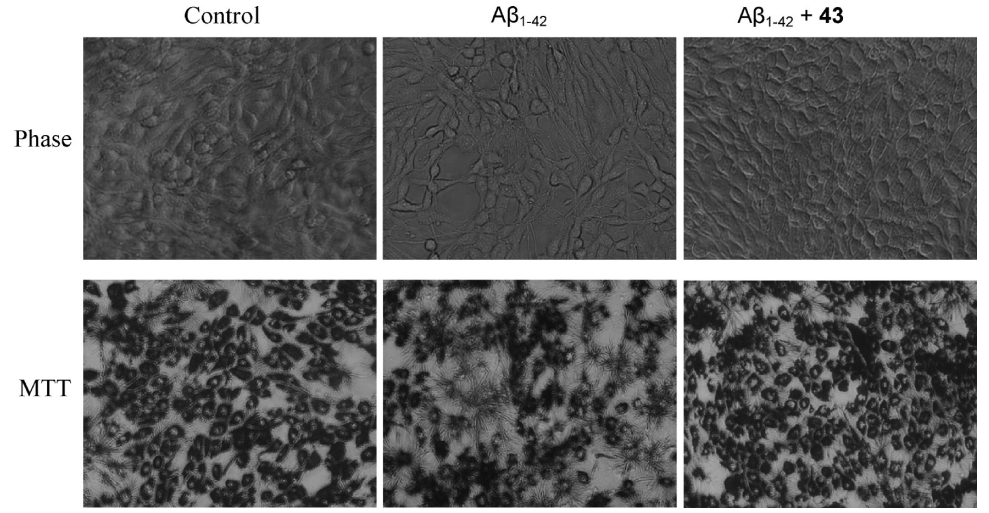

Figure 9. Phase and MTT formazan formation contrast photomicrographs in PC-12 cells treated with 10 μM Aβ_{1-42} and compound **43**. PC-12 cells were incubated with 10 μM Aβ_{1-42}, 10 μM Aβ_{1-42} + 3 μM **43**, or 0.02% DMSO at 37 °C for 48 h, then photographed under a light microscope. Finally MTT was added, and the reaction proceeded for 4 h. Then the samples were photographed.

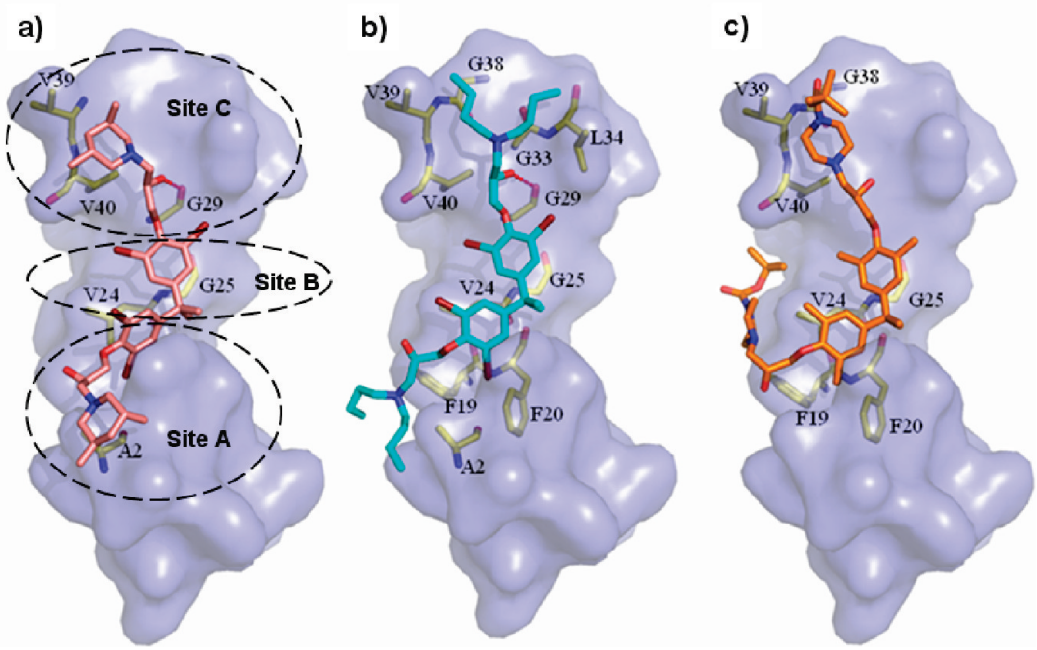

Figure 10. Interactions details of Aβ with compounds **43** (a), **45** (b), and **52** (c) according to the complex model generated by the docking simulation. Aβ is represented as a surface contour, and those residues that hydrophobically interact with inhibitors are shown as yellow sticks.

structures of compounds **43**, **45**, and **52** mainly interact hydrophobically with three sites of Aβ peptide, which are shown in Figure 10. In site A, the phenyl ring of the inhibitor interacts well with the phenyl rings of the residues Tyr10, Phe19, and Phe20 of Aβ. These results are in agreement with the experimental data that the sequence of Aβ_{16-20}, KLVFF, is critically involved in Aβ fibrillation.[35] In site B, in the three complex models, the other phenyl rings of compounds hydrophobically interact with Aβ by Val24, Gly29, and Val40. These results indicated that these residues constituting site A and site B are quite conservative for the inhibitor binding with Aβ, which are also in agreement with the experiment results of the CD assay for compound **43**, and further support the conclusion that some Aβ_{12-28} residues with α-helical conformation could be reverted to β-sheet and β-turn conformations upon interaction with compound **43**. In site C, the hydrophobic ring or alkyl segments of compounds interact with residues Leu34, Gly38, Val39, and Val40, which is also in agreement with the experimental results of Aβ fibrillation.[36] Besides, especially in the case of compound **45**, the more flexible hydrophobic alkyl groups (dibutylamino group) interact much better with the hydrophobic groove constituted by these residues, which partially accounts for the high binding affinity of the inhibitor and demonstrates that introducing flexible substitutents into the molecules is important to improve the inhibitory potency against Aβ aggregation. In addition, that the hydroxyl group of compounds may form hydrogen bonds with the Gly29 and that the inhibitor interacts with the residues of Asp1, Ala2, Glu3 are additional crucial roles for the inhibitory

activity of compounds against Aβ fibrillation. Together, the consistency of the results of our investigations into the binding mode from theoretical results and experimental data further support the rationality of our structure optimization from the parental compound, which will light the way for the discovery of more effective inhibitors against Aβ aggregation.

4. Conclusion

We synthesized and evaluated a series of bisphenol A derivatives as Aβ aggregation inhibitors. Structural optimization for the parental compound **1** led to the synthesis of 34 derivatives. Nine of the synthesized analogues (**40**, **43**−**45**, **47**, and **50**−**53**) demonstrated more effective inhibitory potencies against Aβ aggregation than the parental compound **1**, and five compounds (**22**, **30**, **33, 35**, and **48**) showed equivalent inhibitory potencies against Aβ aggregation compared to the hit compound. Among them, compounds **43**−**45**, **50**, **52**, **53** displayed the most potent inhibitory effects (~5- to 100-fold higher inhibitor potency than that of the hit compound) with IC_{50} values of 0.27−6.2 μM. Structure−activity relationships analysis for all synthesized derivatives indicate that (i) introduction of flexible hydrophobic moieties at the R_3 group is important to improve the inhibitory potencies against Aβ aggregation, and introduction of the rigid segments may lead to a remarkable decrease or loss of inhibitory activities, (ii) four Br atoms on the aryl ring are not absolutely required but may increase the inhibitory potency based on the results of ThT assay. Further investigations showed that compound **43** not only is a more efficient inhibitor against Aβ fibrillation but also exhibits some promising effects in other biological test systems. CD spectroscopy assay indicated that the β-sheet component of Aβ increased in the presence of compound **43**, suggesting that **43** can stabilize the β-sheet conformation by binding to Aβ peptide and further inhibit Aβ fibrillation. Meanwhile, compound **43** not only can dramatically suppress the aggregation of $Aβ_{1-42}$ but also can dissolve the preformed fibrils based on the results of the PICUP and AFM assays. Moreover, experiments assessing the cytotoxicity of compound **43** indicated that it has no toxicity to neuronal cells below 1 μM and can effectively inhibit the $Aβ_{1-42}$-induced neutrotoxicity and increase the cell viability under certain concentrations. Our binding model experiments also demonstrated the consistency of our study on the analysis of binding mode from theoretical results and experimental data, which further support the rationality of our structural optimization. Besides, several compounds (**43** and **52**) also showed good inhibitory effects against γ-secretase. In summary, on the basis of the abilities of these compounds, especially compound **43**, to effectively inhibit Aβ aggregation in various biological assays and even to dissolve the preformed Aβ fibril, these novel chemical structures reported in this study provide a promising potential for therapeutic applications in AD and other types of neurodegenerative disorders.

5. Experimental Section

General Information. The reagents (chemicals) were purchased from a commercial chemical reagent company and used without further purification unless otherwise stated. Analytical thin-layer chromatography (TLC) was done with HSGF 254. All target products were characterized by NMR, LRMS, and HRMS, and all intermediates were characterized by H NMR and LRMS. Chemical shifts were reported in parts per million (ppm, δ) downfield from tetramethylsilane. Proton coupling patterns are described as singlet (s), doublet (d), triplet (t), quartet (q), multipet (m), and broad (br). Low- and high-resolution mass spectra (LRMS and HRMS) were obtained with electric, electrospray, and matrix-assisted laser desorption ionization (EI and ESI) produced by Finnigan MAT-95 and LCQ-DECA spectrometers. An Agilent 1100 series HPLC instrument with an Agilent Zorbax Eclipse XDB-C_{18} (4.6 mm × 150 mm, 5 μm particle size) reversed-phase column was used for analytical HPLC analyses. The elution buffer was an A/B gradient, where A = H_2O and B = CH_3OH. The system conditions were as follows: CH_3OH/H_2O, 85% (v/v) of CH_3OH gradient, flow rate 1.0 mL/min, calculation of the relative purity of each compound at 214 nm. The purity of all tested compounds was above 95%.

General Procedures for the Preparation of Intermediates 2a−c (Intermediate 2a, for Example). To a mixture of 4,4′-(propane-2,2-diyl)bis(2,6-dibromophenol) (**1a**) (5.44 g, 10 mmol) in 8 mL of epichlorohydrin was slowly added powdered KOH (3.0 g, 55 mmol), followed by tetrabutylammonium bromide (0.7 g, 2.2 mmol). The resulting reaction mixture was stirred at room temperature overnight, treated with water, and extracted three times with diethyl ether. The combined organic layers were washed with water and dried by anhydrous Na_2SO_4. After evaporation of the solvent, the residue was purified by silica gel chromatography (petroleum ether (PE)/ethyl acetate (EA) = 4/1) to give 2,2′-(4,4′-(propane-2,2-diyl)bis(2,6-dibromo-4,1-phenylene))-bis (oxy)bis(methylene)dioxirane (**2a**) as a white solid. Yield: 95%. ^{1}H NMR (300 MHz, $CDCl_3$): δ 7.32 (s, 4H), 4.18−4.23 (m, 2H), 4.04−4.10 (m, 2H), 3.47−3.53 (m, 2H), 2.90−2.94 (m, 2H), 2.74−2.77 (m, 2H), 1.61 (s, 6H). ^{13}C NMR (100 MHz, $CDCl_3$): δ 151.0, 148.0, 131.0, 118.0, 74.2, 50.1, 44.8, 42.2, 30.4. LRMS (ESI) m/z 657 $[M + H]^+$.

2,2′-(4,4′-(Propane-2,2-diyl)bis(2-methyl-4,1-phenylene))bis-(oxy)bis(methylene)dioxirane (2b). The intermediate **2b** was prepared from 4,4′-(propane-2,2-diyl)bis(2-methylphenol) (**1b**) and purified by silica gel chromatography (PE/EA = 4/1). Yield: 94%. ^{1}H NMR (300 MHz, $CDCl_3$): δ 7.03−6.96 (m, 4H), 6.70 (t, J = 4.5 Hz, 2H), 4.20 (dd, J = 14.1 Hz, 3.0 Hz, 2H), 3.97 (dd, J = 11.4 Hz, 5.4 Hz, 2H), 3.40−3.33 (m, 2H), 2.93−2.88 (m, 2H), 2.80−2.76 (m, 2H), 2.21 (s, 6H), 1.62 (s, 6H). LRMS (ESI) m/z 369 $[M + H]^+$.

2,2′-(4,4′-(Propane-2,2-diyl)bis(4,1-phenylene))bis(oxy)bis-(methylene)dioxirane (2c). The intermediate **2c** was prepared from 4,4′-(propane-2,2-diyl)diphenol (**1c**) and purified by silica gel chromatography (PE/EA = 4/1). Yield: 98%. ^{1}H NMR (300 MHz, $CDCl_3$): δ 7.16 (d, J = 8.7 Hz, 4H), 6.84 (d, J = 8.7 Hz, 4H), 4.20 (dd, J = 11.1 Hz, 3.3 Hz, 2H), 3.95 (dd, J = 11.1 Hz, 5.7 Hz, 2H), 3.39−3.32 (m, 2H), 2.90 (t, J = 4.5 Hz, 2H), 2.75 (q, J = 2.4 Hz, 2H), 1.65 (s, 6H). LRMS (ESI) m/z 363 $[M + Na]^+$.

4,4′-(Propane-2,2-diyl)bis(2,6-dimethylphenol) (4). To a mixture of concentrated sulfuric acid (98%, 1.5 g, 15 mmol) and acetic acid (1.6 g, 26.7 mmol) was slowly added a solution of 2,6-dimethylphenol (**3**, 37.5 mmol) in acetone (0.44 g, 7.5 mmol), keeping the reaction solution below 15 °C. The resulting mixture was stirred at 15 °C for 1.5 h, diluted with H_2O, and extracted three times with CH_2Cl_2. The combined organic layers were dried by anhydrous Na_2SO_4. After evaporation of the solvent, the residue was purified by silica gel chromatography (PE/EA = 8/1) to give the desirable intermediate **4**. Yield: 58%. ^{1}H NMR (300 MHz, $CDCl_3$): δ 6.84 (s, 4H), 4.45 (s, 2H), 2.21 (s, 12H), 1.60 (s, 6H). LRMS (ESI) m/z 283 $[M - H]^-$.

2,2′-(4,4′-(Propane-2,2-diyl)bis(2,6-dimethyl-4,1-phenylene))-bis(oxy)bis(methylene)dioxirane (5). By the same manner as described for the preparation of **2a**, the intermediate **5** was prepared from the intermediate **4** and epichlorohydrin and purified by silica gel chromatography (PE/EA = 4/1). Yield: 95%. ^{1}H NMR (300 MHz, $CDCl_3$): δ 6.85 (d, J = 8.7 Hz, 4H), 4.04 (dd, J = 11.1 Hz, 3.3 Hz, 2H), 3.76 (dd, J = 11.1 Hz, 6.3 Hz, 2H), 3.40−3.33 (m, 2H), 2.89 (t, J = 4.5 Hz, 2H), 2.72 (q, J = 2.7 Hz, 2H), 2.26 (s, 12H), 1.60 (s, 6H). LRMS (ESI) m/z 419 $[M + Na]^+$.

4,4′-(Perfluoropropane-2,2-diyl)bis(2,6-dibromophenol) (7). To a mixture of compound **6** (2.94 mmol) in acetic acid (5 mL) was slowly added Br_2 (1.88 g, 11.76 mmol). The resulting mixture was stirred at room temperature for 12 h. After evaporation of the solvent, the residue was recrystallized by acetic acid to give pure product. Yield: 92%. ^{1}H NMR (300 MHz, DMSO-d_6): δ 7.39 (s, 4H). LRMS (ESI) m/z 651 $[M - H]^-$.

2,2′-(4,4′-(Perfluoropropane-2,2-diyl)bis(2,6-dibromo-4,1-phenylene))bis(oxy)bis(methylene)dioxirane (8). By the same manner as described for the preparation of **2a**, the intermediate **8** was prepared from the intermediate **7** and epichlorohydrin and purified by silica gel chromatography (PE/EA = 4/1). Yield: 95%. ^{1}H NMR (300 MHz, $CDCl_3$): δ 7.50 (s, 4H), 4.30 (dd, J = 10.8 Hz, 3.9 Hz, 2H), 4.11 (dd, J = 10.8 Hz, 5.7 Hz, 2H), 3.55−3.47 (m, 2H), 2.97−2.90 (m, 2H), 2.79−2.74 (m, 2H). LRMS (ESI) m/z 763 $[M - H]^-$.

2,2′-(4,4′-(Perfluoropropane-2,2-diyl)bis(4,1-phenylene))bis(oxy)-bis(methylene)dioxirane (9). By the same manner as described for the preparation of **2a**, the intermediate **9** was prepared from compound **6** and epichlorohydrin and purified by silica gel chromatography (PE/EA = 4/1). Yield: 90%. ^{1}H NMR (300 MHz, $CDCl_3$): δ 7.31 (d, J=9.0 Hz, 4H), 6.90 (d, J=9.0 Hz, 4H), 4.26 (dd, J = 10.8 Hz, 2.4 Hz, 2H), 3.97 (dd, J = 10.8 Hz, 5.7 Hz, 2H), 3.40−3.34 (m, 2H), 2.95−2.91 (m, 2H), 2.77 (dd, J=4.5 Hz, 2.4 Hz, 2H). ^{13}C NMR (100 MHz, $CDCl_3$): δ 158.6, 131.5, 125.9, 124.3, 114.1, 68.7, 63.6, 50.0, 44.6. LRMS (ESI) m/z 449 $[M + H]^+$.

4,4′-(Ethane-1,1-diyl)bis(2,6-dibromophenol) (11). By the same manner as described for the preparation of **7**, the intermediate **11** was prepared from compound **10**. Yield: 92%. ^{1}H NMR (300 MHz, DMSO-d_6): δ 7.45 (s, 4H), 4.01 (q, J=6.9 Hz, 1H), 1.46 (d, J=7.2 Hz, 3H). LRMS (ESI) m/z 529 $[M - H]^-$.

2,2′-(4,4′-(Ethane-1,1-diyl)bis(2,6-dibromo-4,1-phenylene))bis-(oxy)bis(methylene)dioxirane (12). By the same manner as described for the preparation of **8**, the intermediate **12** was prepared from the intermediate **11** and purified by silica gel chromatography (PE/EA = 4/1). Yield: 95%. ^{1}H NMR (300 MHz, $CDCl_3$): δ 7.30 (s, 4H), 4.19 (dd, J = 10.8 Hz, 3.9 Hz, 2H), 4.04 (dd, J = 10.8 Hz, 5.7 Hz, 2H), 3.96 (q, J=7.2 Hz, 1H), 3.52−3.43 (m, 2H), 2.90 (t, J=4.5 Hz, 2H), 2.74 (dd, J=5.1 Hz, 2.4 Hz, 2H), 1.55 (d, J=7.2 Hz, 3H). LRMS (ESI) m/z 641 $[M - H]^-$.

4,4′-(Cyclopentane-1,1-diyl)diphenol (14). By the same manner as described for the preparation of **4**, the intermediate **14** was prepared from compound **13** and cyclopentanone and purified by silica gel chromatography (PE/EA = 8/1). Yield: 36%. ^{1}H NMR (300 MHz, $CDCl_3$): δ 7.12 (d, J=8.4 Hz, 4H), 6.70 (d, J= 8.4 Hz, 4H), 2.26−2.16 (br, 4H), 1.72−1.65 (br, 4H). LRMS (ESI) m/z 253 $[M - H]^-$.

4,4′-(Cyclopentane-1,1-diyl)bis(2,6-dibromophenol) (15). By the same manner as described for the preparation of **7**, the intermediate **15** was prepared from the intermediate **14** and purified by silica gel chromatography (PE/EA = 4/1). Yield: 92%. ^{1}H NMR (300 MHz, $CDCl_3$): δ 7.28 (s, 4H), 5.76 (s, 2H), 2.19−2.12 (m, 4H), 1.74−1.67 (m, 4H). LRMS (ESI) m/z 569 $[M - H]^-$.

2,2′-(4,4′-(Cyclopentane-1,1-diyl)bis(2,6-dibromo-4,1-phenylene))bis(oxy)bis(methylene)dioxirane (16). By the same manner as described for the preparation of **2a**, the intermediate **16** was prepared from the intermediate **15** and purified by silica gel chromatography (PE/EA = 4/1). Yield: 95%. ^{1}H NMR (300 MHz, $CDCl_3$): δ 7.34 (s, 4H), 4.18 (dd, J=10.2 Hz, 4.2 Hz, 2H), 3.73 (dd, J = 10.2 Hz, 6.0 Hz, 2H), 3.51−3.42 (m, 2H), 2.90 (t, J = 4.8 Hz, 2H), 2.73 (dd, J = 4.8 Hz, 2.4 Hz, 2H), 2.21−2.11 (m, 4H), 1.74−1.64 (m, 4H). LRMS (ESI) m/z 705 $[M + Na]^+$.

4,4′-(Cyclopentane-1,1-diyl)bis(2,6-dimethylphenol) (17a). By the same manner as described for the preparation of **4**, the intermediate **17a** was prepared from 2,6-dimethylphenol (**3**) and cyclopentanone and purified by silica gel chromatography (PE/EA = 8/1). Yield: 42%. ^{1}H NMR (300 MHz, $CDCl_3$): δ 6.87 (s, 4H), 2.20 (s, 12H), 2.19−2.16 (m, 4H), 1.70−1.66 (m, 4H). LRMS (ESI) m/z 309 $[M - H]^-$.

4,4′-(Cyclohexane-1,1-diyl)bis(2,6-dimethylphenol) (17b). By the same manner as described for the preparation of **4**, the intermediate **17b** was prepared from 2,6-dimethylphenol (**3**) and cyclohexanone and purified by silica gel chromatography (PE/EA = 8/1). Yield: 47%. ^{1}H NMR (300 MHz, $CDCl_3$): δ 6.87 (s, 4H), 4.42 (s, 2H), 2.20 (s, 12H), 2.20−2.13 (m, 4H), 1.60−1.42 (m, 6H). LRMS (ESI) m/z 323 $[M - H]^-$.

4,4′-(Cycloheptane-1,1-diyl)bis(2,6-dimethylphenol) (17c). By the same manner as described for the preparation of **4**, the intermediate **17c** was prepared from 2,6-dimethylphenol (**3**) and cycloheptanone and purified by silica gel chromatography (PE/EA = 8/1). Yield: 40%. ^{1}H NMR (300 MHz, $CDCl_3$): δ 6.77 (s, 4H), 4.43 (s, 2H), 2.25−2.21 (m, 4H), 2.20 (s, 12H), 1.73−1.62 (m, 4H), 1.60−1.52 (m, 4H). LRMS (ESI) m/z 337 $[M - H]^-$.

2,2′-(4,4′-(Cyclopentane-1,1-diyl)bis(2,6-dimethyl-4,1-phenylene))bis(oxy)bis(methylene)dioxirane (18a). By the same manner as described for the preparation of **2a**, the intermediate **18a** was prepared from the intermediate **17a** and purified by silica gel chromatography (PE/EA = 4/1). Yield: 95%. ^{1}H NMR (300 MHz, $CDCl_3$): δ 6.87 (s, 4H), 3.99 (dd, J = 10.8 Hz, 3.3 Hz, 2H), 3.73 (dd, J = 10.8 Hz, 6.0 Hz, 2H), 3.39−3.30 (m, 2H), 2.92−2.84 (m, 2H), 2.70 (dd, J=5.1 Hz, 2.4 Hz, 2H), 2.24 (s, 12H), 2.23−2.15 (m, 4H), 1.72−1.61 (m, 4H). LRMS (ESI) m/z 445 $[M + Na]^+$.

2,2′-(4,4′-(Cyclohexane-1,1-diyl)bis(2,6-dimethyl-4,1-phenylene))bis(oxy)bis(methylene)dioxirane (18b). By the same manner as described for the preparation of **2a**, the intermediate **18b** was prepared from the intermediate **17b** and purified by silica gel chromatography (PE/EA = 4/1). Yield: 95%. ^{1}H NMR (300 MHz, $CDCl_3$): δ 6.87 (s, 4H), 4.00 (dd, J = 11.4 Hz, 3.3 Hz, 2H), 3.74 (dd, J=10.8 Hz, 5.7 Hz, 2H), 3.38−3.31 (m, 2H), 2.88 (t, J=4.5 Hz, 2H), 2.70 (dd, J=5.4 Hz, 2.4 Hz, 2H), 2.24 (s, 12H), 2.21−2.14 (m, 4H), 1.60−1.42 (m, 6H). LRMS (ESI) m/z 437 $[M + H]^+$.

2,2′-(4,4′-(Cycloheptane-1,1-diyl)bis(2,6-dimethyl-4,1-phenylene))bis(oxy)bis(methylene)dioxirane (18c). By the same manner as described for the preparation of **2a**, the intermediate **18c** was prepared from the intermediate **17c** and purified by silica gel chromatography (PE/EA = 4/1). Yield: 95%. ^{1}H NMR (300 MHz, $CDCl_3$): δ 6.76 (s, 4H), 4.01 (dd, J = 11.1 Hz, 3.3 Hz, 2H), 3.76 (dd, J = 11.1 Hz, 5.7 Hz, 2H), 3.38−3.32 (m, 2H), 2.90−2.86 (m, 2H), 2.71 (dd, J = 5.4 Hz, 3.0 Hz, 2H), 2.23 (s, 12H), 2.22−2.17 (m, 4H), 1.72−1.61 (m, 4H), 1.60−1.52 (m, 4H). LRMS (ESI) m/z 451 $[M + H]^+$.

4,4′-(Cyclohexane-1,1-diyl)bis(2-bromophenol) (20). To a mixture of compound **19** (2.94 mmol) in acetic acid (5 mL) was slowly added Br_2 (0.94 g, 5.88 mmol). The resulting mixture was stirred at room temperature for 12 h. After evaporation of the solvent, the residue was recrystallized by acetic acid to give pure product. Yield: 90%. ^{1}H NMR (300 MHz, $CDCl_3$): δ 7.33 (d, J=2.4 Hz, 2H), 7.10 (dd, J=8.4 Hz, 2.4 Hz, 2H), 6.83 (d, J=8.4 Hz, 2H), 5.36 (s, 2H), 2.21−2.13 (m, 4H), 1.60−1.43 (m, 6H). LRMS (ESI) m/z 425 $[M - H]^-$.

2,2′-(4,4′-(Cyclohexane-1,1-diyl)bis(2-bromo-4,1-phenylene))-bis(oxy)bis(methylene)dioxirane (21). By the same manner as described for the preparation of **2a**, the intermediate **21** was prepared from the intermediate **20** and purified by silica gel chromatography (PE/EA = 4/1). Yield: 95%. ^{1}H NMR (300 MHz, $CDCl_3$): δ 7.42 (d, J=2.4 Hz, 2H), 7.09 (dd, J=8.4 Hz, 2.4 Hz, 2H), 6.83 (d, J=8.4 Hz, 2H), 4.25 (dd, J=11.1 Hz, 3.0 Hz, 2H), 4.03 (dd, J=11.1 Hz, 5.1 Hz, 2H), 3.41−3.34 (m, 2H), 2.91 (t, J=4.5 Hz, 2H), 2.70 (dd, J=5.1 Hz, 2.4 Hz, 2H), 2.20−2.13 (m, 4H), 1.55−1.47 (m, 6H). LRMS (ESI) m/z 561 $[M + Na]^+$.

General Procedures for the Preparation of the Target Compounds 1, 22, 25−28, 43−46 (Compound 1, for Example). To a mixture of **2a** (1.64 g, 2.5 mmol) in 10 mL of CH_3OH was added morpholine (0.26 g, 3 mmol). The resulting mixture was stirred and heated to reflux for 3 h. Then the reaction mixture was cooled, diluted with H_2O, and extracted three times with ethyl acetate. The combined organic layers were dried by anhydrous Na_2SO_4. After evaporation of the solvent, the residue was purified by silica gel chromatography (CH_2Cl_2/CH_3OH = 20/1) to give the target

compound 3,3′-(4,4′-(propane-2,2-diyl)bis(2,6-dibromo-4,1-phenylene))bis(oxy)bis(1- morpholinopropan-2-ol) (**1**). Yield: 79%. ^{1}H NMR (300 MHz, $CDCl_3$): δ 7.31 (s, 4H), 4.18−4.23 (m, 2H), 4.06−4.11 (m, 4H), 3.73−3.76 (m, 8H), 2.64−3.73 (m, 8H), 2.50−2.55 (m, 4H), 1.61 (s, 6H). ^{13}C NMR (100 MHz, $CDCl_3$): δ 150.9, 147.9, 131.0, 118.0, 74.9, 67.0, 66.0, 60.9, 53.8, 42.2, 30.4. LRMS (EI) m/z 830 (M^+). HRMS (EI) m/z calcd $C_{29}H_{38}Br_4N_2O_6$ (M^+) 825.9463, found 825.9453.

3,3′-(4,4′-(Propane-2,2-diyl)bis(2,6-dibromo-4,1-phenylene))bis(oxy)bis(1-(4-methylpiperazin-1-yl)propan-2-ol) (22). By the same manner as described for the preparation of **1**, compound **22** was prepared from 1-methylpiperazine and purified by silica gel chromatography (CH_2Cl_2/CH_3OH = 20/1). Yield: 80%. ^{1}H NMR (300 MHz, $CDCl_3$): δ 7.30 (s, 4H), 4.16−4.21 (m, 2H), 4.04−4.08 (m, 4H), 2.56−2.77 (m, 20H), 2.34 (s, 6H), 1.60 (s, 6H). ^{13}C NMR (100 MHz, $CDCl_3$): δ 150.8, 147.9, 131.0, 118.0, 74.9, 66.1, 60.2, 54.9, 45.7, 42.2, 30.4. LRMS (EI) m/z 856 (M^+). HRMS (EI) m/z calcd $C_{31}H_{44}Br_4N_4O_4$ (M^+) 852.0096, found 852.0055.

3,3′-(4,4′-(Propane-2,2-diyl)bis(2,6-dimethyl-4,1-phenylene))bis(oxy)bis(1-morpholinopropan-2-ol) (23). By the same manner as described for the preparation of **1**, compound **23** was prepared from the intermediate **5** and morpholine and purified by silica gel chromatography (CH_2Cl_2/CH_3OH = 20/1). Yield: 80%. ^{1}H NMR (300 MHz, $CDCl_3$): δ 6.83 (s, 4H), 4.13−4.08 (m, 2H), 3.80 (d, J = 5.1 Hz, 4H), 3.73 (t, 8H), 2.71−2.63 (m, 4H), 2.62−2.57 (m, 4H), 2.53−2.44 (m, 4H), 2.24 (s, 12H), 1.59 (s, 6H). ^{13}C NMR (100 MHz, $CDCl_3$): δ 153.0, 146.1, 129.7, 127.2, 73.7, 66.9, 66.1, 61.0, 53.7, 41.7, 31.0, 16.5. LRMS (EI) m/z 570 $[M]^+$. HRMS (EI) m/z calcd for $C_{33}H_{50}N_2O_6$ $[M]^+$ 570.3669, found 570.3681.

3,3′-(4,4′-(Propane-2,2-diyl)bis(2,6-dimethyl-4,1-phenylene))bis(oxy)bis(1-(4-methylpiperazin-1-yl)propan-2-ol) (24). By the same manner as described for the preparation of **1**, compound **24** was prepared from the intermediate **5** and 1-methylpiperazine and purified by silica gel chromatography (CH_2Cl_2/CH_3OH = 20/1). Yield: 78%. ^{1}H NMR (300 MHz, $CDCl_3$): δ 6.82 (s, 4H), 4.11−4.06 (m, 2H), 3.78 (d, J = 4.8 Hz, 4H), 2.73−2.44 (m, 20H), 2.31 (s, 6H), 2.23 (s, 12H), 1.58 (s, 6H). ^{13}C NMR (100 MHz, $CDCl_3$): δ 153.1, 146.1, 129.7, 127.2, 73.9, 66.4, 60.4, 55.1, 53.5, 45.9, 41.7, 31.0, 16.5. LRMS (EI) m/z 596 $[M]^+$. HRMS (EI) m/z calcd for $C_{35}H_{56}N_4O_4$ $[M]^+$ 596.4302, found 596.4301.

3,3′-(4,4′-(Propane-2,2-diyl)bis(2-methyl-4,1-phenylene))bis(oxy)bis(1-morpholinopropan-2-ol) (25). By the same manner as described for the preparation of **1**, compound **25** was prepared from the intermediate **2b** and morpoline and purified by silica gel chromatography (CH_2Cl_2/CH_3OH = 20/1). Yield: 80%. ^{1}H NMR (300 MHz, $CDCl_3$): δ 7.03−6.97 (m, 4H), 6.72 (d, J = 8.7 Hz, 2H), 4.18−4.11 (m, 2H), 4.01−3.91 (m, 4H), 3.76−3.69 (m, 8H), 3.70−3.61 (m, 4H), 2.57 (d, J = 6.6 Hz, 4H), 2.52−2.43 (m, 4H), 2.19 (s, 6H), 1.62 (s, 6H). ^{13}C NMR (100 MHz, $CDCl_3$): δ 154.5, 143.1, 129.3, 125.9, 124.7, 110.3, 70.1, 67.0, 65.5, 61.3, 53.8, 41.5, 31.1, 16.5. LRMS (EI) m/z 542 $[M]^+$. HRMS (EI) m/z calcd for $C_{31}H_{46}N_2O_6$ $[M]^+$ 542.3356, found 542.3360.

3,3′-(4,4′-(Propane-2,2-diyl)bis(4,1-phenylene))bis(oxy)bis(1-morpholinopropan-2-ol) (26). By the same manner as described for the preparation of **1**, compound **26** was prepared from the intermediate **2c** and morpoline and purified by silica gel chromatography (CH_2Cl_2/CH_3OH = 20/1). Yield: 79%. ^{1}H NMR (300 MHz, $CDCl_3$): δ 7.09 (d, J = 8.7 Hz, 4H), 6.78 (d, J = 8.7 Hz, 4H), 4.12−4.01 (m, 2H), 3.93 (d, J = 5.1 Hz, 4H), 3.68 (m, 8H), 2.65−2.55 (m, 4H), 2.53−2.48 (m, 4H), 2.48−2.38 (m, 4H), 1.60 (s, 6H). ^{13}C NMR (100 MHz, $CDCl_3$): δ 156.4, 143.4, 127.7, 113.8, 70.0, 66.9, 65.3, 61.0, 53.7, 41.6, 31.0. LRMS (EI) m/z 514 $[M]^+$. HRMS (EI) m/z calcd for $C_{29}H_{42}N_2O_6$ $[M]^+$ 514.3043, found 514.3047.

3,3′-(4,4′-(Propane-2,2-diyl)bis(4,1-phenylene))bis(oxy)bis(1-(4-methylpiperazin-1-yl)propan-2-ol) (27). By the same manner as described for the preparation of **1**, compound **27** was prepared from the intermediate **2c** and 1-methylpiperazine and purified by silica gel chromatography (CH_2Cl_2/CH_3OH = 20/1). Yield: 75%. ^{1}H NMR (300 MHz, $CDCl_3$): δ 7.10 (d, J = 8.7 Hz, 4H), 6.79 (d, J = 8.7 Hz, 4H), 4.11−4.01 (m, 2H), 3.94 (d, J = 4.8 Hz, 4H), 2.78−2.64 (m, 4H), 2.60−2.40 (m, 16H), 2.30 (s, 6H), 1.61 (s, 6H). ^{13}C NMR (100 MHz, $CDCl_3$): δ 156.4, 143.3, 127.6, 113.8, 70.1, 65.4, 60.4, 55.1, 53.5, 46.0, 41.6, 31.0. LRMS (EI) m/z 540 $[M]^+$. HRMS (EI) m/z calcd for $C_{31}H_{48}N_4O_4$ $[M]^+$ 540.3676, found 540.3673.

3,3′-(4,4′-(Propane-2,2-diyl)bis(4,1-phenylene))bis(oxy)bis(1-(piperidin-1-yl)propan-2-ol) (28). By the same manner as described for the preparation of **1**, compound **28** was prepared from the intermediate **2c** and piperidine and purified by silica gel chromatography (CH_2Cl_2/CH_3OH = 20/1). Yield: 85%. ^{1}H NMR (300 MHz, $CDCl_3$): δ 7.10 (d, J = 8.7 Hz, 4H), 6.80 (d, J = 8.7 Hz, 4H), 4.10−4.00 (m, 2H), 3.94−3.90 (m, 4H), 2.62−2.52 (br, 4H), 2.45 (d, J = 6.3 Hz, 4H), 2.40−2.30 (br, 4H), 1.60 (s, 6H), 1.59−1.51 (m, 8H), 1.44−1.39 (m, 4H). ^{13}C NMR (100 MHz, $CDCl_3$): δ 156.5, 143.3, 127.7, 113.8, 70.2, 65.2, 61.3, 54.7, 41.7, 31.0, 25.8, 24.0. LRMS (EI) m/z 510 $[M]^+$. HRMS (EI) m/z calcd for $C_{31}H_{46}N_2O_4$ $[M]^+$ 510.3458, found 510.3431.

3,3′-(4,4′-(Perfluoropropane-2,2-diyl)bis(2,6-dibromo-4,1-phenylene))bis(oxy)bis(1-morpholinopropan-2-ol) (29). By the same manner as described for the preparation of **1**, compound **29** was prepared from the intermediate **8** and morpholine and purified by silica gel chromatography (CH_2Cl_2/CH_3OH = 20/1). Yield: 80%. ^{1}H NMR (300 MHz, $CDCl_3$): δ 7.49 (s, 4H), 4.27−4.18 (m, 2H), 4.17−4.13 (m, 4H), 3.75 (m, 8H), 2.74−2.65 (m, 8H), 2.57−2.47 (m, 4H). ^{13}C NMR (100 MHz, $CDCl_3$): δ 154.0, 134.2, 130.5, 123.3, 118.4, 75.1, 67.0, 65.9, 60.8, 53.8. LRMS (EI) m/z 938 $[M]^+$. HRMS (EI) m/z calcd for $C_{29}H_{32}Br_4F_6N_2O_6$ $[M]^+$ 933.8898, found 933.8785.

3,3′-(4,4′-(Perfluoropropane-2,2-diyl)bis(2,6-dibromo-4,1-phenylene))bis(oxy)bis(1-(4-methylpiperazin-1-yl)propan-2-ol) (30). By the same manner as described for the preparation of **1**, compound **30** was prepared from the intermediate **8** and 1-methylpiperazine and purified by silica gel chromatography (CH_2Cl_2/CH_3OH = 20/1). Yield: 78%. ^{1}H NMR (300 MHz, $CDCl_3$): δ 7.47 (s, 4H), 4.25−4.15 (m, 2H), 4.12 (m, 4H), 2.79−2.69 (m, 4H), 2.68−2.43 (m, 16H), 2.31 (s, 6H). ^{13}C NMR (100 MHz, $CDCl_3$): δ 154.1, 134.2, 130.5, 123.3, 118.4, 75.2, 66.1, 60.1, 55.0, 53.4, 45.9. LRMS (EI) m/z 964 $[M]^+$. HRMS (EI) m/z calcd for $C_{31}H_{38}Br_4F_6N_4O_6$ $[M]^+$ 959.9531, found 959.9486.

3,3′-(4,4′-(Perfluoropropane-2,2-diyl)bis(4,1-phenylene))bis(oxy)bis(1-morpholinopropan-2-ol) (31). By the same manner as described for the preparation of **1**, compound **31** was prepared from the intermediate **9** and morpholine and purified by silica gel chromatography (CH_2Cl_2/CH_3OH = 20/1). Yield: 80%. ^{1}H NMR (300 MHz, $CDCl_3$): δ 7.30 (d, J = 8.7 Hz, 4H), 6.90 (d, J = 9.3 Hz, 4H), 4.21−4.12 (m, 2H), 4.02 (d, J = 5.1 Hz, 4H), 3.81−3.74 (m, 8H), 2.78−2.68 (m, 4H), 2.64−2.50 (m, 4H), 2.59−2.49 (m, 4H). ^{13}C NMR (100 MHz, $CDCl_3$): δ 158.8, 131.4, 125.7, 125.6, 114.0, 70.1, 66.9, 65.3, 63.4, 61.0, 53.7. LRMS (EI) m/z 622 $[M]^+$. HRMS (EI) m/z calcd for $C_{29}H_{36}F_6N_2O_6$ $[M]^+$ 622.2478, found 622.2486.

3,3′-(4,4′-(Perfluoropropane-2,2-diyl)bis(4,1-phenylene))bis(oxy)bis(1-(4-methylpiperazin-1-yl)propan-2-ol) (32). By the same manner as described for the preparation of **1**, compound **32** was prepared from the intermediate **9** and 1-methylpiperazine and purified by silica gel chromatography (CH_2Cl_2/CH_3OH = 20/1). Yield: 78%. ^{1}H NMR (300 MHz, $CDCl_3$): δ 7.27 (d, J = 8.4 Hz, 4H), 6.87 (d, J = 9.0 Hz, 4H), 4.13−4.03 (m, 2H), 3.98 (d, J = 4.5 Hz, 4H), 2.69 (br, 4H), 2.61−2.35 (m, 16H), 2.27 (s, 6H). ^{13}C NMR (100 MHz, $CDCl_3$): δ 158.8, 131.4, 125.7, 122.9, 114.0, 70.2, 65.3, 60.3, 55.1, 53.3, 46.0. LRMS (EI) m/z 648 $[M]^+$. HRMS (EI) m/z calcd for $C_{31}H_{42}F_6N_4O_4$ $[M]^+$ 648.3110, found 648.3114.

3,3′-(4,4′-(Ethane-1,1-diyl)bis(2,6-dibromo-4,1-phenylene))bis(oxy)bis(1-(4-methylpiperazin-1-yl)propan-2-ol) (33). By the same manner as described for the preparation of **1**, compound **33** was prepared from the intermediate **12** and 1-methylpiperazine and purified by silica gel chromatography (CH_2Cl_2/CH_3OH = 20/1). Yield: 78%. ^{1}H NMR (300 MHz, $CDCl_3$): δ 7.30 (s, 4H),

4.21−4.15 (m, 2H), 4.08−4.04 (m, 4H), 3.98−3.95 (m, 1H), 2.74−2.52 (m, 20H), 2.33 (s, 6H), 1.56 (d, J = 6.9 Hz, 3H). ^{13}C NMR (100 MHz, $CDCl_3$): δ 151.2, 143.5, 131.6, 118.2, 74.9, 66.1, 60.2, 55.0, 52.5, 45.9, 42.6, 21.4. LRMS (EI) m/z 842 $[M]^+$. HRMS (EI) m/z calcd for $C_{30}H_{42}Br_4N_4O_4$ $[M]^+$ 837.9940, found 837.9894.

3,3′-(4,4′-(Cyclopentane-1,1-diyl)bis(2,6-dibromo-4,1-phenylene))bis(oxy)bis(1-morpholinopropan-2-ol) (34). By the same manner as described for the preparation of **1**, compound **34** was prepared from the intermediate **16** and morpholine and purified by silica gel chromatography (CH_2Cl_2/CH_3OH = 20/1). Yield: 80%. ^{1}H NMR (300 MHz, $CDCl_3$): δ 7.32 (s, 4H), 4.23−4.14 (m, 2H), 4.05 (m, 4H), 3.73 (t, 8H), 2.72−2.63 (m, 8H), 2.56−2.46 (m, 4H), 2.20−2.13 (br, 4H), 1.73−1.67 (br, 4H). ^{13}C NMR (100 MHz, $CDCl_3$): δ 150.9, 146.2, 131.2, 118.0, 75.0, 67.0, 66.2, 61.0, 54.7, 53.8, 38.6, 22.6. LRMS (EI) m/z 856 $[M]^+$. HRMS (EI) m/z calcd for $C_{31}H_{40}Br_4N_2O_6$ $[M]^+$ 851.9620, found 851.9620.

3,3′-(4,4′-(Cyclopentane-1,1-diyl)bis(2,6-dibromo-4,1-phenylene))bis(oxy)bis(1-(4-methylpiperazin-1-yl)propan-2-ol) (35). By the same manner as described for the preparation of **1**, compound **35** was prepared from the intermediate **16** and 1-methylpiperazine and purified by silica gel chromatography (CH_2Cl_2/CH_3OH = 20/1). Yield: 78%. ^{1}H NMR (300 MHz, $CDCl_3$): δ 7.31 (s, 4H), 4.20−4.11 (m, 2H), 4.06−4.01 (m, 4H), 2.75−2.61 (m, 8H), 2.60−2.35 (m, 12H), 2.89 (s, 6H), 2.19−2.13 (br, 4H), 1.73−1.66 (br, 4H). ^{13}C NMR (100 MHz, $CDCl_3$): δ 151.0, 146.2, 131.2, 118.0, 75.1, 66.3, 60.3, 55.2, 54.7, 53.3, 46.0, 38.6, 22.6. LRMS (EI) m/z 882 $[M]^+$. HRMS (EI) m/z calcd for $C_{33}H_{46}Br_4N_4O_4$ $[M]^+$ 878.0253, found 878.0290.

3,3′-(4,4′-(Cyclopentane-1,1-diyl)bis(2,6-dimethyl-4,1-phenylene))bis(oxy)bis(1-morpholinopropan-2-ol) (36). By the same manner as described for the preparation of **1**, compound **36** was prepared from the intermediate **18a** and morpholine and purified by silica gel chromatography (CH_2Cl_2/CH_3OH = 20/1). Yield: 80%. ^{1}H NMR (300 MHz, $CDCl_3$): δ 6.87 (s, 4H), 4.12−4.04 (m, 2H), 3.78−3.68 (m, 12H), 2.69−2.62 (m, 4H), 2.60−2.55 (m, 4H), 2.50−2.45 (m, 4H), 2.23 (s, 12H), 2.19 (br, 4H), 1.65 (br, 4H). ^{13}C NMR (100 MHz, $CDCl_3$): δ 152.9, 144.3, 129.7, 127.4, 73.7, 66.9, 66.2, 61.1, 54.5, 53.8, 38.8, 22.9, 16.5. LRMS (EI) m/z 596 $[M]^+$. HRMS (EI) m/z calcd for $C_{35}H_{52}N_2O_6$ $[M]^+$ 596.3825, found 596.3818.

3,3′-(4,4′-(Cyclopentane-1,1-diyl)bis(2,6-dimethyl-4,1-phenylene))bis(oxy)bis(1-(4-methylpiperazin-1-yl)propan-2-ol) (37). By the same manner as described for the preparation of **1**, compound **37** was prepared from the intermediate **18a** and 1-methylpiperazine and purified by silica gel chromatography (CH_2Cl_2/CH_3OH = 20/1). Yield: 78%. ^{1}H NMR (300 MHz, $CDCl_3$): δ 6.85 (s, 4H), 4.09−4.03 (m, 2H), 3.75 (d, J = 4.8 Hz, 4H), 2.70−2.43 (m, 20H), 2.28 (s, 6H), 2.22 (s, 12H), 2.18 (br, 4H), 1.64 (br, 4H). ^{13}C NMR (100 MHz, $CDCl_3$): δ 153.0, 144.3, 129.7, 127.3, 73.8, 66.3, 60.3, 55.1, 54.5, 46.0, 38.7, 22.9, 16.5. LRMS (EI) m/z 622 $[M]^+$. HRMS (EI) m/z calcd for $C_{37}H_{58}N_4O_4$ $[M]^+$ 622.4458, found 622.4462.

3,3′-(4,4′-(Cyclohexane-1,1-diyl)bis(2,6-dimethyl-4,1-phenylene))bis(oxy)bis(1-morpholinopropan-2-ol) (38). By the same manner as described for the preparation of **1**, compound **38** was prepared from the intermediate **18b** and morpholine and purified by silica gel chromatography (CH_2Cl_2/CH_3OH = 20/1). Yield: 80%. ^{1}H NMR (300 MHz, $CDCl_3$): δ 6.87 (s, 4H), 4.13−4.08 (m, 2H), 3.78 (d, J = 4.8 Hz, 4H), 3.74 (t, 8H), 2.72−2.63 (m, 4H), 2.62−2.58 (m, 4H), 2.53−2.46 (m, 4H), 2.24 (s, 12H), 2.18 (br, 4H), 1.51 (br, 6H). ^{13}C NMR (100 MHz, $CDCl_3$): δ 152.8, 144.0, 129.8, 127.5, 73.7, 67.0, 66.2, 61.0, 53.7, 45.0, 37.2, 26.4, 22.9, 16.6. LRMS (EI) m/z 610 $[M]^+$. HRMS (EI) m/z calcd for $C_{36}H_{54}N_2O_6$ $[M]^+$ 610.3982, found 610.3990.

3,3′-(4,4′-(Cyclohexane-1,1-diyl)bis(2,6-dimethyl-4,1-phenylene))bis(oxy)bis(1-(4-methylpiperazin-1-yl)propan-2-ol) (39). By the same manner as described for the preparation of **1**, compound **39** was prepared from the intermediate **18b** and 1-methylpiperazine and purified by silica gel chromatography (CH_2Cl_2/CH_3OH = 20/1). Yield: 78%. ^{1}H NMR (300 MHz, $CDCl_3$): δ 6.85 (s, 4H), 4.10−4.04 (m, 2H), 3.76 (d, J = 5.1 Hz, 4H), 2.71−2.44 (m, 20H), 2.30 (s, 6H), 2.23 (s, 12H), 2.17 (br, 4H), 1.50 (br, 6H). ^{13}C NMR (100 MHz, $CDCl_3$): δ 152.7, 143.7, 129.6, 127.3, 73.8, 66.3, 60.3, 54.9, 53.0, 45.7, 44.7, 37.1, 26.2, 22.7, 16.4. LRMS (EI) m/z 636 $[M]^+$. HRMS (EI) m/z calcd for $C_{38}H_{60}N_4O_4$ $[M]^+$ 636.4615, found 636.4612.

3,3′-(4,4′-(Cyclohexane-1,1-diyl)bis(2-bromo-4,1-phenylene))bis(oxy)bis(1-(4-methylpiperazin-1-yl)propan-2-ol) (40). By the same manner as described for the preparation of **1**, compound **40** was prepared from the intermediate **21** and 1-methylpiperazine and purified by silica gel chromatography (CH_2Cl_2/CH_3OH = 20/1). Yield: 78%. ^{1}H NMR (300 MHz, $CDCl_3$): δ 7.41 (d, J = 1.8 Hz, 2H), 7.09 (dd, J = 8.7 Hz, 1.8 Hz, 2H), 6.82 (d, J = 8.7 Hz, 2H), 4.13 (m, 2H), 4.01 (m, 4H), 2.54−2.76 (m, 22H), 2.34 (s, 6H), 2.17 (br, 4H), 1.50 (br, 6H). ^{13}C NMR (100 MHz, $CDCl_3$): δ 152.7, 142.3, 131.7, 127.1, 113.2, 112.1, 71.3, 65.6, 60.3, 54.9, 53.1, 45.8, 44.8, 37.0, 26.0, 22.6. LRMS (EI) m/z 738 $[M]^+$. HRMS (EI) m/z calcd for $C_{34}H_{50}Br_2N_4O_4$ $[M]^+$ 736.2199, found 736.2195.

3,3′-(4,4′-(Cycloheptane-1,1-diyl)bis(2,6-dimethyl-4,1-phenylene))bis(oxy)bis(1-morpholinopropan-2-ol) (41). By the same manner as described for the preparation of **1**, compound **41** was prepared from the intermediate **18c** and morpholine and purified by silica gel chromatography (CH_2Cl_2/CH_3OH = 20/1). Yield: 80%. ^{1}H NMR (300 MHz, $CDCl_3$): δ 6.75 (s, 4H) 4.12−4.07 (m, 2H), 3.78 (d, J = 5.1 Hz, 4H), 3.73 (t, 8H), 2.70−2.63 (m, 4H), 2.61−2.56 (m, 4H), 2.52−2.45 (m, 4H), 2.22 (s, 12H), 2.18 (br, 4H), 1.66 (br, 4H), 1.56 (br, 4H). ^{13}C NMR (100 MHz, $CDCl_3$): δ 152.6, 146.5, 129.5, 127.6, 73.7, 66.9, 66.2, 61.0, 53.7, 48.8, 40.3, 30.2, 24.3, 16.6. LRMS (EI) m/z 624 $[M]^+$. HRMS (EI) m/z calcd for $C_{37}H_{56}N_2O_6$ $[M]^+$ 624.4138, found 624.4116.

3,3′-(4,4′-(Cycloheptane-1,1-diyl)bis(2,6-dimethyl-4,1-phenylene))bis(oxy)bis(1-(4-methylpiperazin-1-yl)propan-2-ol) (42). By the same manner as described for the preparation of **1**, compound **42** was prepared from the intermediate **18c** and 1-methylpiperazine and purified by silica gel chromatography (CH_2Cl_2/CH_3OH = 20/1). Yield: 78%. ^{1}H NMR (300 MHz, $CDCl_3$): δ 6.74 (s, 4H), 4.12−4.02 (m, 2H), 3.77 (d, J = 5.1 Hz, 4H), 2.70−2.42 (m, 20H), 2.29 (s, 6H), 2.21 (s, 12H), 2.18 (br, 4H), 1.65 (br, 4H), 1.54 (br, 4H). ^{13}C NMR (100 MHz, $CDCl_3$): δ 152.7, 146.4, 129.6, 127.6, 73.8, 66.3, 60.4, 55.1, 53.5, 48.8, 46.0, 40.3, 30.2, 24.3, 16.6. LRMS (EI) m/z 650 $[M]^+$. HRMS (EI) m/z calcd for $C_{39}H_{62}N_4O_4$ $[M]^+$ 650.4771, found 650.4781.

3,3′-(4,4′-(Propane-2,2-diyl)bis(2,6-dibromo-4,1-phenylene))bis(oxy)bis(1-(3,5-dimethylpiperidin-1-yl)propan-2-ol) (43). By the same manner as described for the preparation of **1**, compound **43** was prepared from 3,5-dimethylpiperidine and purified by silica gel chromatography (CH_2Cl_2/CH_3OH = 20/1). Yield: 75%. ^{1}H NMR (300 MHz, $CDCl_3$): δ 7.27 (s, 4H), 4.38 (m, 2H), 4.05 (m, 4H), 2.93 (m, 8H), 1.90 (s, 8H), 1.58 (s, 6H), 1.01 (m, 4H), 0.88 (m, 12H). ^{13}C NMR (100 MHz, $CDCl_3$): δ 150.0, 148.4, 131.1, 117.2, 74.4, 63.8, 59.7, 57.8, 42.0, 38.6, 29.5, 28.1, 18.3. LRMS (ESI) m/z 883 $[M + H]^+$. HRMS (ESI) m/z calcd $C_{35}H_{51}Br_4N_2O_4$ $[M + H]^+$ 879.0582, found 879.0563.

3,3′-(4,4′-(Propane-2,2-diyl)bis(2,6-dibromo-4,1-phenylene))bis(oxy)bis(1-(1,4-dioxa-8-azaspiro[4.5]decan-8-yl)propan-2-ol) (44). By the same manner as described for the preparation of **1**, compound **44** was prepared from 1,4-dioxa-8-azaspiro[4.5]decane and purified by silica gel chromatography (CH_2Cl_2/CH_3OH = 20/1). Yield: 75%. ^{1}H NMR (300 MHz, $CDCl_3$): δ 7.30 (s, 4H), 4.15−4.18 (m, 2H), 4.08 (d, J = 5.1 Hz, 4H), 3.97 (s, 8H), 2.74−2.80 (m, 4H), 2.68 (d, J = 6.6 Hz, 4H), 2.56−2.61 (m, 4H), 1.75−1.79 (m, 8H), 1.60 (s, 6H). ^{13}C NMR (100 MHz, $CDCl_3$): δ 151.0, 147.9, 131.0, 118.0, 107.0, 75.0, 66.3, 64.2, 59.9, 51.6, 42.2, 34.9, 30.4. LRMS (ESI) m/z 943 $[M + H]^+$. HRMS (ESI) m/z calcd $C_{35}H_{47}Br_4N_2O_8$ $[M + H]^+$ 939.0066, found 939.0060.

3,3′-(4,4′-(Propane-2,2-diyl)bis(2,6-dibromo-4,1-phenylene))bis(oxy)bis(1-(dibutylamino)propan-2-ol) (45). By the same manner as described for the preparation of **1**, compound **45** was prepared from 1,4-dioxa-8-azaspiro[4.5]decane and purified by

silica gel chromatography ($CH_2Cl_2/CH_3OH = 20/1$). Yield: 79%. ^1H NMR (300 MHz, $CDCl_3$): δ 7.29 (s, 4H), 4.18−4.23 (m, 2H), 4.03−4.10 (m, 4H), 2.52−2.87 (m, 12H), 1.59 (s, 6H), 1.47−1.54 (m, 8H), 1.28−1.39 (m, 8H), 0.84−0.95 (m, 12H). ^{13}C NMR (100 MHz, $CDCl_3$): δ 151.0, 147.9, 131.0, 118.0, 74.8, 66.1, 57.6, 54.1, 42.2, 30.5, 29.7, 20.5, 14.0. LRMS (ESI) m/z 915 $[M + H]^+$. HRMS (ESI) m/z calcd $C_{37}H_{59}Br_4N_2O_4$ $[M + H]^+$ 911.1208, found 911.1219.

3,3′-(4,4′-(Propane-2,2-diyl)bis(2,6-dibromo-4,1-phenylene))bis(oxy)bis(1-(4-*tert*-butylphenylamino)propan-2-ol) (46). By the same manner as described for the preparation of **1**, compound **46** was prepared from 4-*tert*-butylphenylamine and purified by silica gel chromatography ($CH_2Cl_2/CH_3OH = 20/1$). Yield: 60%. ^1H NMR (300 MHz, $CDCl_3$): δ 7.32 (s, 4H), 7.21−7.25 (d, $J = 8.7$ Hz, 4H), 6.64−6.68 (d, $J = 8.7$ Hz, 4H), 4.28−4.31 (m, 2H), 4.15−4.22 (m, 4H), 3.46−3.52 (m, 2H), 3.32−3.39 (m, 2H), 1.61 (s, 6H), 1.39 (s, 18H). ^{13}C NMR (100 MHz, $CDCl_3$): δ 150.6, 148.1, 145.6, 140.8, 131.1, 126.1, 117.9, 113.1, 75.2, 69.1, 46.7, 42.3, 33.9, 31.5, 30.5. LRMS (EI) m/z 954 $[M]^+$. HRMS (EI) m/z calcd for $C_{41}H_{50}Br_4N_2O_4$ $[M]^+$ 954.0463, found 954.0453.

3,3′-(4,4′-(Propane-2,2-diyl)bis(2,6-dimethyl-4,1-phenylene))bis(oxy)bis(1-(3,5-dimethylpiperidin-1-yl)propan-2-ol) (47). By the same manner as described for the preparation of **1**, compound **47** was prepared from the intermediate **5** and 3,5-dimethylpiperidine and purified by silica gel chromatography (CH_2Cl_2/CH_3OH = 20/1). Yield: 82%. ^1H NMR (300 MHz, $CDCl_3$): δ 6.83 (s, 4H), 4.15−4.05 (m, 2H), 3.78 (d, $J = 5.1$ Hz, 4H), 2.98−2.92 (m, 2H), 2.81−2.78 (m, 2H), 2.57−2.45 (m, 5H), 2.25 (s, 12H), 1.84−1.47 (m, 15H), 0.98 (d, $J = 6.6$ Hz, 2H), 0.88−0.85 (m, 10H), 0.59−0.54 (m, 2H). ^{13}C NMR (100 MHz, $CDCl_3$): δ 153.2, 146.0, 129.7, 127.2, 74.1, 66.2, 63.1, 60.5, 41.9, 41.7, 31.2, 31.0, 19.4, 16.5. LRMS (EI) m/z 622 $[M]^+$. HRMS (EI) m/z calcd for $C_{39}H_{62}N_2O_4$ $[M]^+$ 622.4710, found 622.4695.

3,3′-(4,4′-(Propane-2,2-diyl)bis(2,6-dimethyl-4,1-phenylene))bis(oxy)bis(1-(1,4-dioxa-8-azaspiro[4.5]decan-8-yl)propan-2-ol) (48). By the same manner as described for the preparation of **1**, compound **48** was prepared from the intermediate **5** and 1,4-dioxa-8-azaspiro[4.5]decane and purified by silica gel chromatography ($CH_2Cl_2/CH_3OH = 20/1$). Yield: 80%. ^1H NMR (300 MHz, $CDCl_3$): δ 6.82 (s, 4H), 4.11−4.02 (m, 2H), 4.96−3.94 (m, 8H), 3.78 (d, $J = 4.8$ Hz, 4H), 2.81−2.70 (m, 4H), 2.62−2.50 (m, 8H), 2.23 (s, 12H), 1.76 (m, 8H), 1.58 (s, 6H). ^{13}C NMR (100 MHz, $CDCl_3$): δ 153.1, 146.0, 129.7, 127.1, 106.9, 73.9, 66.5, 64.2, 60.0, 51.5, 41.7, 34.9, 31.0, 16.5. LRMS (EI) m/z 682 $[M]^+$. HRMS (EI) m/z calcd for $C_{39}H_{58}N_2O_8$ $[M]^+$ 682.4193, found 682.4168.

3,3′-(4,4′-(Propane-2,2-diyl)bis(2,6-dimethyl-4,1-phenylene))bis(oxy)bis(1-(piperidin-1-yl)propan-2-ol) (49). By the same manner as described for the preparation of **1**, compound **49** was prepared from the intermediate **5** and piperidine and purified by silica gel chromatography ($CH_2Cl_2/CH_3OH = 20/1$). Yield: 82%. ^1H NMR (300 MHz, $CDCl_3$): δ 6.83 (s, 4H), 4.14−4.03 (m, 2H), 3.79 (d, $J = 4.8$ Hz, 4H), 2.68−2.58 (m, 4H), 2.53 (d, $J = 6.6$ Hz, 4H), 2.46−2.35 (m, 4H), 2.24 (s, 12H), 1.64−1.56 (m, 14H), 1.51−1.42 (m, 4H). ^{13}C NMR (100 MHz, $CDCl_3$): δ 153.2, 146.0, 129.7, 127.1, 74.1, 66.2, 61.2, 54.7, 41.6, 31.0, 26.0, 24.2, 16.5. LRMS (EI) m/z 566 $[M]^+$. HRMS (EI) m/z calcd for $C_{35}H_{54}N_2O_4$ $[M]^+$ 566.4084, found 566.4048.

3,3′-(4,4′-(Propane-2,2-diyl)bis(2,6-dimethyl-4,1-phenylene))bis(oxy)bis(1-(azepan-1-yl)propan-2-ol) (50). By the same manner as described for the preparation of **1**, compound **50** was prepared from the intermediate **5** and azepane and purified by silica gel chromatography (CH_2Cl_2/CH_3OH = 20/1). Yield: 82%. ^1H NMR (300 MHz, $CDCl_3$): δ 6.83 (s, 4H), 4.04−3.95 (m, 2H), 3.79 (d, $J = 5.1$ Hz, 4H), 2.84−2.76 (m, 6H), 2.74−2.56 (m, 6H), 2.25 (s, 12H), 1.72−1.56 (m, 22H). ^{13}C NMR (100 MHz, $CDCl_3$): δ 153.3, 146.0, 129.7, 127.2, 74.1, 66.8, 60.7, 55.9, 41.9, 31.0, 28.4, 26.9, 16.5. LRMS (EI) m/z 594 $[M]^+$. HRMS (EI) m/z calcd for $C_{37}H_{58}N_2O_4$ $[M]^+$ 594.4397, found 594.4373.

3,3′-(4,4′-(Propane-2,2-diyl)bis(2,6-dimethyl-4,1-phenylene))bis(oxy)bis(1-(pyrrolidin-1-yl)propan-2-ol) (51). By the same manner as described for the preparation of **1**, compound **51** was prepared from the intermediate **5** and pyrrolidine and purified by silica gel chromatography ($CH_2Cl_2/CH_3OH = 20/1$). Yield: 82%. ^1H NMR (300 MHz, $CDCl_3$): δ 6.83 (s, 4H), 4.12−4.05 (m, 2H), 3.79 (d, $J = 4.8$ Hz, 4H), 2.89−2.80 (m, 2H), 2.74−2.68 (m, 4H), 2.64−2.55 (m, 6H), 2.24 (s, 12H), 1.85−1.78 (m, 8H), 1.59 (s, 6H). ^{13}C NMR (100 MHz, $CDCl_3$): δ 153.1, 146.0, 129.7, 127.1, 74.0, 68.1, 58.6, 54.2, 41.7, 31.0, 23.6, 16.5. LRMS (EI) m/z 538 $[M]^+$. HRMS (EI) m/z calcd for $C_{33}H_{50}N_2O_4$ $[M]^+$ 538.3771, found 538.3740.

***tert*-Butyl 4,4′-(3,3′-(4,4′-(Propane-2,2-diyl)bis(2,6-dimethyl-4,1-phenylene))bis(oxy)bis(2-hydroxypropane-3,1-diyl))dipiperazine-1-carboxylate (52).** By the same manner as described for the preparation of **1**, compound **52** was prepared from the intermediate **5** and 1-bocpiperazine and purified by silica gel chromatography (CH_2Cl_2/CH_3OH = 20/1). Yield: 75%. ^1H NMR (300 MHz, $CDCl_3$): δ 6.82 (s, 4H), 4.14−4.07 (m, 2H), 3.79 (d, $J = 5.1$ Hz, 4H), 3.45 (t, 8H), 2.68−2.57 (m, 8H), 2.48−2.38 (m, 4H), 2.23 (s, 12H), 1.58 (s, 6H), 1.45 (s, 18H). ^{13}C NMR (100 MHz, $CDCl_3$): δ 154.6, 153.0, 146.1, 129.7, 127.2, 79.8, 73.7, 66.3, 60.7, 53.1, 41.7, 31.0, 28.4, 16.5. LRMS (EI) m/z 768 $[M]^+$. HRMS (EI) m/z calcd for $C_{43}H_{68}N_4O_8$ $[M]^+$ 768.5037, found 768.5040.

3,3′-(4,4′-(Propane-2,2-diyl)bis(2,6-dimethyl-4,1-phenylene))bis(oxy)bis(1-(4-benzylpiperazin-1-yl)propan-2-ol) (53). By the same manner as described for the preparation of **1**, compound **53** was prepared from the intermediate **5** and 1-benzylpiperazine and purified by silica gel chromatography (CH_2Cl_2/CH_3OH = 20/1). Yield: 77%. ^1H NMR (300 MHz, $CDCl_3$): δ 7.26−7.17 (m, 10H), 6.75 (s, 4H), 4.05−3.96 (m, 2H), 3.71 (d, $J = 4.5$ Hz, 4H), 3.45 (s, 4H), 2.64−2.43 (m, 20H), 2.16 (s, 12H), 1.52 (s, 6H). ^{13}C NMR (100 MHz, $CDCl_3$): δ 153.1, 146.0, 138.0, 129.7, 129.2, 128.2, 127.2, 127.0, 74.0, 66.3, 63.0, 60.5, 53.1, 53.1, 41.7, 31.0, 16.5. LRMS (EI) m/z 748 $[M]^+$. HRMS (EI) m/z calcd for $C_{47}H_{64}N_4O_4$ $[M]^+$ 748.4928, found 748.4938.

3,3′-(4,4′-(Propane-2,2-diyl)bis(2,6-dimethyl-4,1-phenylene))bis(oxy)bis(1-(3,5-dimethylphenylamino)propan-2-ol) (54). By the same manner as described for the preparation of **1**, compound **54** was prepared from the intermediate **5** and 3,5-dimethylphenylamine and purified by silica gel chromatography (CH_2Cl_2/CH_3OH = 20/1). Yield: 73%. ^1H NMR (300 MHz, $CDCl_3$): δ 6.88 (s, 4H), 6.44 (s, 2H), 6.36 (s, 4H), 4.31−4.21 (m, 2H), 3.90 (d, $J = 4.8$ Hz, 4H), 3.50−3.43 (m, 2H), 3.34−3.26 (m, 2H), 2.28 (s, 12H), 2.27 (s, 12H), 1.63 (s, 6H). ^{13}C NMR (100 MHz, $CDCl_3$): δ 152.8, 148.1, 146.3, 139.0, 129.6, 127.3, 120.0, 111.3, 73.9, 69.4, 46.8, 41.7, 31.0, 21.5, 16.6. LRMS (EI) m/z 638 $[M]^+$. HRMS (EI) m/z calcd for $C_{41}H_{54}N_2O_4$ $[M]^+$ 638.4084, found 638.4094.

3,3′-(4,4′-(Propane-2,2-diyl)bis(2,6-dimethyl-4,1-phenylene))bis(oxy)bis(1-(4-*tert*-butylphenylamino)propan-2-ol) (55). By the same manner as described for the preparation of **1**, compound **55** was prepared from the intermediate **5** and 4-*tert*-butylphenylamine and purified by silica gel chromatography (CH_2Cl_2/CH_3OH = 20/1). Yield: 73%. ^1H NMR (300 MHz, $CDCl_3$): δ 7.25 (d, J = 7.8 Hz, 4H), 6.87 (s, 4H), 6.67 (d, $J = 8.1$ Hz, 4H), 4.30−4.22 (m, 2H), 3.90 (d, $J = 4.5$ Hz, 4H), 3.50−3.27 (m, 4H), 2.27 (s, 12H), 1.62 (s, 6H), 1.31 (s, 18H). ^{13}C NMR (100 MHz, $CDCl_3$): δ 152.8, 146.3, 145.6, 140.9, 129.7, 127.3, 126.1, 113.2, 73.9, 69.4, 47.2, 41.7, 33.86, 31.5, 31.0, 16.6. LRMS (EI) m/z 694 $[M]^+$. HRMS (EI) m/z calcd for $C_{45}H_{62}N_2O_4$ $[M]^+$ 694.4710, found 694.4713.

Acknowledgment. We gratefully acknowledge financial support from CAS Introducing Outstanding Oversea Scientists Project, the National Natural Science Foundation of China (Grants 20721003, 20872153, and 30670425), the Ministry of Science and Technology (Grants 2009CB940900, 2006AA020602, and 2008AA02Z138), and National S&T Major Projects (2009ZX09301-001, 2009ZX09501-001, and 2009ZX09501-010).

Supporting Information Available: HPLC results for the purity check of all tested compounds and the details of γ-secretase fluorogenic substrate assay. This material is available free of charge via the Internet at http://pubs.acs.org.

References

(1) Haass, C.; De Strooper, B. The presenilins in Alzheimer's disease—proteolysis holds the key. *Science* **1999**, *286*, 916–919.
(2) Geula, C.; Wu, C. K.; Saroff, D.; Lorenzo, A.; Yuan, M.; Yankner, B. A. Aging renders the brain vulnerable to amyloid beta-protein neurotoxicity. *Nat. Med.* **1998**, *4*, 827–831.
(3) Austen, B. M.; Paleologou, K. E.; Ali, S. A.; Qureshi, M. M.; Allsop, D.; El-Agnaf, O. M. Designing peptide inhibitors for oligomerization and toxicity of Alzheimer's beta-amyloid peptide. *Biochemistry* **2008**, *47*, 1984–1992.
(4) Liu, D.; Xu, Y.; Feng, Y.; Liu, H.; Shen, X.; Chen, K.; Ma, J.; Jiang, H. Inhibitor discovery targeting the intermediate structure of beta-amyloid peptide on the conformational transition pathway: implications in the aggregation mechanism of beta-amyloid peptide. *Biochemistry* **2006**, *45*, 10963–10972.
(5) Hasegawa, T.; Ukai, W.; Jo, D. G.; Xu, X.; Mattson, M. P.; Nakagawa, M.; Araki, W.; Saito, T.; Yamada, T. Homocysteic acid induces intraneuronal accumulation of neurotoxic Abeta42: implications for the pathogenesis of Alzheimer's disease. *J. Neurosci. Res.* **2005**, *80*, 869–876.
(6) Billings, L. M.; Oddo, S.; Green, K. N.; McGaugh, J. L.; LaFerla, F. M. Intraneuronal Abeta causes the onset of early Alzheimer's disease-related cognitive deficits in transgenic mice. *Neuron* **2005**, *45*, 675–688.
(7) Yadav, A.; Sonker, M. Perspectives in designing anti aggregation agents as Alzheimer disease drugs. *Eur. J. Med. Chem.* **2009**, *44*, 3866–3873.
(8) Bolognesi, M. L.; Banzi, R.; Bartolini, M.; Cavalli, A.; Tarozzi, A.; Andrisano, V.; Minarini, A.; Rosini, M.; Tumiatti, V.; Bergamini, C.; Fato, R.; Lenaz, G.; Hrelia, P.; Cattaneo, A.; Recanatini, M.; Melchiorre, C. Novel class of quinone-bearing polyamines as multi-target-directed ligands to combat Alzheimer's disease. *J. Med. Chem.* **2007**, *50*, 4882–4897.
(9) Selkoe, D. J. Alzheimer's disease: genes, proteins, and therapy. *Physiol. Rev.* **2001**, *81*, 741–766.
(10) Iwatsubo, T.; Odaka, A.; Suzuki, N.; Mizusawa, H.; Nukina, N.; Ihara, Y. Visualization of A beta 42(43) and A beta 40 in senile plaques with end-specific A beta monoclonals: evidence that an initially deposited species is A beta 42(43). *Neuron* **1994**, *13*, 45–53.
(11) Suzuki, N.; Cheung, T. T.; Cai, X. D.; Odaka, A.; Otvos, L., Jr.; Eckman, C.; Golde, T. E.; Younkin, S. G. An increased percentage of long amyloid beta protein secreted by familial amyloid beta protein precursor (beta APP717) mutants. *Science* **1994**, *264*, 1336–1340.
(12) Dahlgren, K. N.; Manelli, A. M.; Stine, W. B., Jr.; Baker, L. K.; Krafft, G. A.; LaDu, M. J. Oligomeric and fibrillar species of amyloid-beta peptides differentially affect neuronal viability. *J. Biol. Chem.* **2002**, *277*, 32046–32053.
(13) Selkoe, D. J. Translating cell biology into therapeutic advances in Alzheimer's disease. *Nature* **1999**, *399*, A23–A31.
(14) Klein, W. L.; Krafft, G. A.; Finch, C. E. Targeting small Abeta oligomers: the solution to an Alzheimer's disease conundrum? *Trends Neurosci.* **2001**, *24*, 219–224.
(15) Lansbury, P. T., Jr. Inhibition of amyloid formation: a strategy to delay the onset of Alzheimer's disease. *Curr. Opin. Chem. Biol.* **1997**, *1*, 260–267.
(16) Talaga, P. Beta-amyloid aggregation inhibitors for the treatment of Alzheimer's disease: dream or reality? *Mini-Rev. Med. Chem.* **2001**, *1*, 175–186.
(17) Estrada, L. D.; Soto, C. Disrupting beta-amyloid aggregation for Alzheimer disease treatment. *Curr. Top. Med. Chem.* **2007**, *7*, 115–126.
(18) Doig, A. J. Peptide inhibitors of beta-amyloid aggregation. *Curr. Opin. Drug Discovery Dev.* **2007**, *10*, 533–539.
(19) Matharu, B.; Gibson, G.; Parsons, R.; Huckerby, T. N.; Moore, S. A.; Cooper, L. J.; Millichamp, R.; Allsop, D.; Austen, B. Galantamine inhibits beta-amyloid aggregation and cytotoxicity. *J. Neurol. Sci.* **2009**, *280*, 49–58.
(20) Rocha, S.; Cardoso, I.; Borner, H.; Pereira, M. C.; Saraiva, M. J.; Coelho, M. Design and biological activity of beta-sheet breaker peptide conjugates. *Biochem. Biophys. Res. Commun.* **2009**, *380*, 397–401.
(21) Adessi, C.; Soto, C. Converting a peptide into a drug: strategies to improve stability and bioavailability. *Curr. Med. Chem.* **2002**, *9*, 963–978.
(22) Xu, Y.; Shen, J.; Luo, X.; Zhu, W.; Chen, K.; Ma, J.; Jiang, H. Conformational transition of amyloid beta-peptide. *Proc. Natl. Acad. Sci. U.S.A.* **2005**, *102*, 5403–5407.
(23) Lee, K. H.; Shin, B. H.; Shin, K. J.; Kim, D. J.; Yu, J. A hybrid molecule that prohibits amyloid fibrils and alleviates neuronal toxicity induced by beta-amyloid (1−42). *Biochem. Biophys. Res. Commun.* **2005**, *328*, 816–823.
(24) Sun, Y.; Marz, P.; Otten, U.; Ge, J.; Rose-John, S. The effect of gp130 stimulation on glutamate-induced excitotoxicity in primary hippocampal neurons. *Biochem. Biophys. Res. Commun.* **2002**, *295*, 532–539.
(25) Varghese, J. N.; Smith, P. W.; Sollis, S. L.; Blick, T. J.; Sahasrabudhe, A.; McKimm-Breschkin, J. L.; Colman, P. M. Drug design against a shifting target: a structural basis for resistance to inhibitors in a variant of influenza virus neuraminidase. *Structure* **1998**, *6*, 735–746.
(26) Morris, G. M.; Goodsell, D. S.; Halliday, R. S.; Huey, R.; Hart, W. E.; Belew, R. K.; Olson, A. J. Automated docking using a Lamarckian genetic algorithm and an empirical binding free energy function. *J. Comput. Chem.* **1998**, *19*, 1639–1662.
(27) LeVine, H., 3rd. Thioflavine T interaction with synthetic Alzheimer's disease beta-amyloid peptides: detection of amyloid aggregation in solution. *Protein Sci.* **1993**, *2*, 404–410.
(28) Barrow, C. J.; Yasuda, A.; Kenny, P. T.; Zagorski, M. G. Solution conformations and aggregational properties of synthetic amyloid beta-peptides of Alzheimer's disease. Analysis of circular dichroism spectra. *J. Mol. Biol.* **1992**, *225*, 1075–1093.
(29) Jarvet, J.; Damberg, P.; Bodell, K.; Goran Eriksson, L. E.; Graslund, A. Reversible random coil to β-sheet transition and the early stage of aggregation of the Aβ(12−28) fragment from the Alzheimer peptide. *J. Am. Chem. Soc.* **2000**, *122*, 4261–4268.
(30) Qin, X. R.; Abe, H.; Nakanishi, H. NMR and CD studies on the interaction of Alzheimer beta-amyloid peptide (12−28) with beta-cyclodextrin. *Biochem. Biophys. Res. Commun.* **2002**, *297*, 1011–1015.
(31) Danielsson, J.; Jarvet, J.; Damberg, P.; Graslund, A. Two-site binding of beta-cyclodextrin to the Alzheimer Abeta(1−40) peptide measured with combined PFG-NMR diffusion and induced chemical shifts. *Biochemistry* **2004**, *43*, 6261–6269.
(32) Bitan, G.; Lomakin, A.; Teplow, D. B. Amyloid beta-protein oligomerization: prenucleation interactions revealed by photo-induced cross-linking of unmodified proteins. *J. Biol. Chem.* **2001**, *276*, 35176–35184.
(33) Ono, K.; Hasegawa, K.; Naiki, H.; Yamada, M. Anti-amyloidogenic activity of tannic acid and its activity to destabilize Alzheimer's beta-amyloid fibrils in vitro. *Biochim. Biophys. Acta* **2004**, *1690*, 193–202.
(34) Baba, K.; Okada, K.; Kinoshita, T.; Imaoka, S. Bisphenol A disrupts Notch signaling by inhibiting gamma-secretase activity and causes eye dysplasia of *Xenopus laevis*. *Toxicol. Sci.* **2009**, *108*, 344–355.
(35) Tjernberg, L. O.; Naslund, J.; Lindqvist, F.; Johansson, J.; Karlstrom, A. R.; Thyberg, J.; Terenius, L.; Nordstedt, C. Arrest of beta-amyloid fibril formation by a pentapeptide ligand. *J. Biol. Chem.* **1996**, *271*, 8545–8548.
(36) Fulop, L.; Zarandi, M.; Datki, Z.; Soos, K.; Penke, B. Beta-amyloid-derived pentapeptide RIIGLa inhibits Abeta(1−42) aggregation and toxicity. *Biochem. Biophys. Res. Commun.* **2004**, *324*, 64–69.